scientific reports

OPEN

Enhanced artificial hummingbird algorithm with chaotic traversal flight

Juan Du[1,2], Jilong Zhang[1,2✉], Shouliang Li[1] & Zhen Yang[1]

Tackling the shortcomings of slow convergence, imprecision, and entrapment in local optima inherent in traditional meta-heuristic algorithms, this study presents the enhanced artificial hummingbird algorithm with chaotic traversal flight (CEAHA), which employs chaotic ergodicity within the foundational framework of the conventional artificial hummingbird algorithm. This approach implements chaotic motion within local regions of the solution space, ensuring a thorough exploration of potential optima and preventing algorithmic stagnation at local maxima by guaranteeing a non-repetitive traversal of all search states. This study also analyzes the intrinsic mechanisms by which eight different chaotic mappings affect optimization performance, from the perspectives of invariant measures and traversal efficiency of ergodic chaotic motion. In comparative tests with 21 meta-heuristic algorithms on the CEC2014, CEC2019, and CEC2022 benchmark suites across various dimensions, CEAHA demonstrates superior optimization performance. Furthermore, the practicability and robustness of CEAHA have been confirmed in mechanical design optimization problems through 4 engineering instances: pressure vessel, gear trains, speed reducers, and piston levers.

Keywords Meta-heuristic optimization, Chaos, Artificial hummingbird algorithm, Mechanical design optimization

Meta-heuristic optimization algorithms, simulating natural or biological behaviors, aim to effectively avoid local optima and achieve global ones. They outperform in handling a range of complex decision-making scenarios involving nonlinear, high-dimensional, non-convex variables such as path planning, resource allocation, neural network architecture search, optimal control, and parameter identification. For instance, the enhanced sand cat swarm optimization algorithm (ESCSO)[1] that combines adaptive social neighborhood search with Lévy flights is used to improve the accuracy and response speed of unmanned aerial vehicle (UAV) path planning and real-time obstacle avoidance, enhance the quality of samples generated under the interfered fluid dynamical system, and find optimal weights and biases for multi-layer perceptrons. The basic behavioral rules of Boids model[2]-separation, alignment, and cohesion-are merged with deep reinforcement learning to develop a control framework for UAV pursuit-evasion in dynamic and complex environments. A multi-objective particle swarm optimization algorithm addresses distribution issues during refined oil shortages, minimizing operational costs and maximizing gas station satisfaction[3]. IEGQO-AOA[4], building on the original AOA, effectively addresses practical engineering design problems of solar photovoltaic parameter extraction by integrating information exchange, adaptive Gaussian distribution, and quasi-opposition based learning. Additionally, more effective strategies for optimizing PID controller gains include an improved stochastic fractal search algorithm (ISFS)[5] with a piecewise linear chaotic map (PLCM), an improved symbiotic organisms search algorithm (ISOS)[6] integrating quasi-oppositional based learning with chaotic local search, and a modified salp swarm algorithm (mSSA)[7] that adds chaotic map, leader information exchange, and randomness to enhance diversity. Notably, ISOS and mSSA have also shown exceptional performance in solving constrained engineering problems such as compression springs, pressure vessels, automatic voltage regulators, and cantilever beams. Moreover, meta-heuristic optimization algorithms, depending on their simulation objects and methodologies[8,9], can be classified into four main categories (Fig. 1): evolution-based, physics-based, human-based and swarm-based methods. Evolution-based algorithms are inspired by Darwin and Mendel's theories of natural evolution, simulating the selection and reproduction processes of biological entities in their environment. Some of the most popular algorithms are genetic algorithm (GA)[10], differential evolution (DE)[11], genetic programming (GP)[12], evolutionary mating algorithm (EMA)[13], gene expression programming (GEP)[14]. And some enhanced versions of DE are also

[1]School of Information Science and Engineering, Lanzhou University, Lanzhou 730000, China. [2]These authors contributed equally: Juan Du and Jilong Zhang. ✉email: 15136170774@163.com
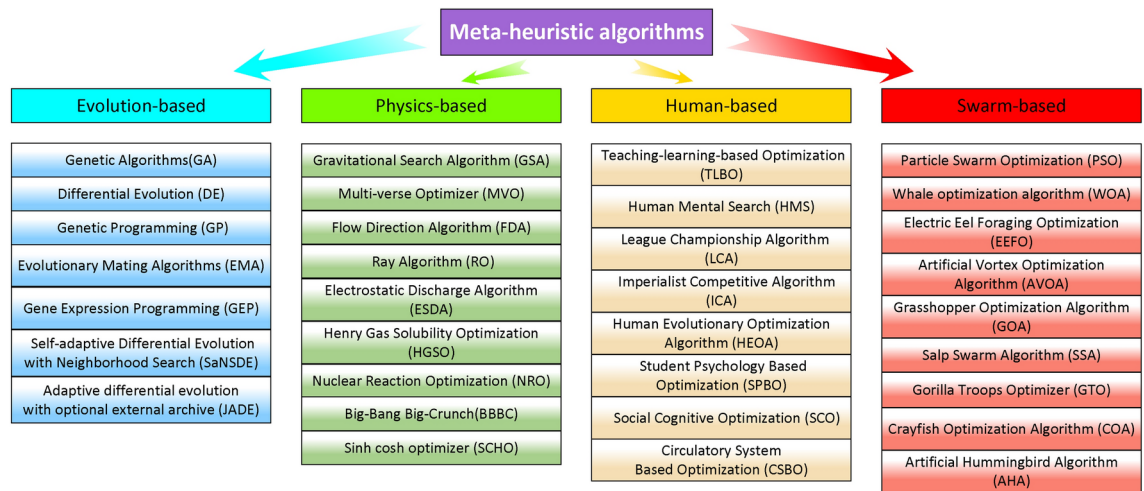
Figure 1. Classification of meta-heuristic optimization algorithms.

widely used in engineering optimal design, such as self-adaptive differential evolution with neighborhood search (SaNSDE)[15] and adaptive differential evolution with optional external archive (JADE)[16].

Physics-based optimization algorithms mimic certain rules and phenomena observed within physical systems. Some of the most widely accepted algorithms are gravitational search algorithm (GSA)[17], multi-verse optimizer (MVO)[18], flow direction algorithm (FDA)[19], ray optimization (RO)[20], electrostatic discharge algorithm (ESDA)[21], Henry gas solubility optimization (HGSO)[22], nuclear reaction optimization (NRO)[23], big-bang big-crunch (BBBC)[24] and sinh cosh optimizer (SCHO)[25,26].

Human-based algorithms attempt to construct global optimization mechanisms by utilizing characteristics of human social and cognitive activities. Some of the most typical algorithms are teaching-learning-based optimization (TLBO)[27], human mental search (HMS)[28], league championship algorithm (LCA)[29], imperialist competitive algorithm (ICA)[30], human evolutionary optimization algorithm (HEOA)[31], student psychology based optimization (SPBO)[32], social cognitive optimization (SCO)[33] and circulatory system based optimization (CSBO)[34].

Swarm-based methods attempt to simulate the habitat, foraging, survival laws and movement characteristics of biological communities. Some of the most popular algorithms are particle swarm optimization (PSO)[35], whale optimization algorithm (WOA)[36], electric eel foraging optimization (EEFO)[37], artificial vortex optimization algorithm (AVOA)[38], grasshopper optimization algorithm (GOA)[39], salp swarm algorithm (SSA)[40], gorilla troops optimizer (GTO)[41], crayfish optimization algorithm (COA)[42] and the recently emerged artificial hummingbird algorithm (AHA)[43].

The artificial hummingbird algorithm (AHA), stands out in the meta-heuristic realm through its unique bionic approach. Emulating hummingbird-flights and foraging strategies, AHA enables agents to explore and exploit the solution space with some efficiency. Distinctively, agents in AHA possess a memory system to track their visits to other hummingbirds' locations, highlighting intelligent behavior. With fewer control parameters, AHA offers simplicity and flexibility, making it widely used in various applications, such as new energy system design[44], the coordinated scheduling of wind-solar-thermal generation[45], and searching for neural network optimal architectures[46]. Yet, AHA still faces difficulties achieving precision and convergence in non-convex, high-dimensional complex problems with a wide search domain[47].

It's worth noting that balancing exploration and exploitation represents a critical challenge in meta-heuristic algorithm design[48,49]. Exploration, driven by diversity, is essential for surveying the search space and pinpointing probable zones for optimal solutions. Conversely, exploitation involves intensive probing within these zones to hasten convergence to the optimum. Lack of exploration may weaken performance and risk local optima traps, whereas poor exploitation may impair the precise pinpointing of the best solution. Employing chaos theory has emerged as a favored method for refining heuristic algorithms to overcome this dilemma[50,51].

Chaos is a type of deterministic nonlinear system with aperiodic behavior characterized by extreme sensitivity to initial conditions, rendering long-term prediction impractical[52]. It has been widely applied in various scientific disciplines, such as the design of pseudo-random number generators, construction of chaotic neural networks, and establishment of secure communication[53]. Earlier studies indicated that the global search capacities of certain chaotic sequences have been highly effective in enhancing the performance of metaheuristic optimization algorithms[54,55]. For example, a chaotic enhanced adaptive hybrid butterfly particle swarm optimization algorithm[56] and an improved chaotic nonlinear dynamic inertia weight PSO algorithm[57] have been utilized for target localization and secure path planning, respectively. Chaotic motion facilitates the traversal of every state around attractors, allowing meta-heuristic algorithms to explore more extensively and avoid local optima. Based on these properties, the chaotic optimization algorithm (COA) was proposed, utilizing the Logistic map[58]. This strategy underwent further refinement in 2018, resulting in the creation of the niche chaotic optimization algorithm (NCOA)[59], which partitions the entire solution space into smaller parts to facilitate chaotic search within each parts. Some studies have developed new search strategies by alternating

the search behavior of COA with traditional meta-heuristic algorithms, thereby enhancing solution quality. For instance, ISOS[6] employed PLCM with a uniform invariant probability density to perform chaotic local search (CLS) around the globally optimal individual, naturally reducing the search radius as iterations progress. Compared to the original SOS, ISOS only added one parameter-the number of CLS iterations-yet significantly improved performance. Similarly, accelerated particle swarm optimization with chaotic search (APSOC)[60], by examining the impact of ten different chaotic maps on iterative search, found that integrating Circle map with APSO yielded better optimization results. However, this approach required adjustments to the chaotic search radius and shrinkage coefficient, complicating the parameter tuning process. Furthermore, chaotic evolution (CE)[61,62] was developed to simulate the rapid blending and diffusive movements of chaos in the process of crossover and mutation of intelligent individuals, leading to faster convergence.

Additionally, integrating chaotic sequences into traditional meta-heuristic algorithms could increase population diversity and prevent premature convergence. Such strategies were implemented in several algorithms, including the chaotic dwarf mongoose optimization algorithm (CDMO) for feature selection[63], the chaotic African vultures optimization algorithm (CAOVA)[64] for achieving optimal power flow with real devices and stochastic wind power, and the chaotic Runge Kutta optimization (CRUN) for solving constrained engineering problems[65]. Specifically, ISFS[5] analyzed the impact of Logistic, PLCM, Iterative, and Sine maps on the first statistical process of the original SFS and found that PLCM notably enhanced population diversity and facilitated a smooth transition from exploration to exploitation, effectively optimizing automatic generation control in power systems. In mSSA[7], the main control parameter for exploration and exploitation underwent systematic, ergodic chaotic changes through the embedding of a sinusoidal map, ensuring that the algorithm maintained an effective balance between exploration and exploitation from the first to the last iteration.

Although various chaotic systems have been applied to explore solution spaces, it remains unclear which types possess superior search efficiency or are better suited for optimization strategy design. Additionally, the underlying mechanisms of chaotic optimization warrant further investigation to ensure continuous advancement in theoretical design.

The No Free Lunch Theorem of Optimization[66] theorizes that it is impossible for any single algorithm to effectively solve all optimization problems, and such an algorithm will never emerge. This theorem motivates ongoing innovation and the proposal of more efficient meta-heuristic optimization techniques. Recently, some enhanced versions of the AHA algorithm incorporating chaos theory have been proposed, such as DGSAHA algorithm[67], which is based on the golden sine factor and integrates the concepts of differential evolution crossover and mutation; LCAHA algorithm[47], which combines Lévy flight and sinusoidal chaotic map; and IAHA algorithm[68], which utilizes Chebyshev map for population initialization settings. These researches all employ chaotic sequences generated from chaotic maps to determine initial population positions. Furthermore, other algorithmic designs, such as the chaotic whale optimization algorithm (CWOA)[69], hyper-chaos cuckoo search (HCS)[70], demonstrate that relying solely on pseudo-random sequences from chaos maps for initializing population positions can enhance optimization performance. However, the limitations of these enhancement strategies are evident in their failure to effectively utilize chaotic maps during the exploration and exploitation phases of the algorithm. Additionally, in real-world engineering optimization instances, most heuristic algorithms may encounter diminished performance or weakened convergence. Hence, to address various engineering scenarios, there is an ongoing requirement to refine and advance optimization strategies.

Motivated by the factors mentioned above, this paper introduces an innovative chaotic optimization strategy grounded in the classical AHA algorithm - namely, the enhanced artificial hummingbird with chaotic traversal flight (CEAHA). An in-depth examination of the invariant probability measures and traversal efficiency within chaotic sequences is conducted, aiming to reveal how different chaotic maps fundamentally influence the optimization performance of meta-heuristic algorithms. This further expands the research frontier concerning the chaotic motion of intelligent agents within the field of optimization algorithms. The novelties and primary contributions of CEAHA are as follows:

- The concept of a chaotic traversal efficiency has been introduced as a novel metric based on spatial ergodicity to delve into the internal mechanics of chaotic optimization.
- A novel strategy for chaotic optimization has been developed, integrating a chaos traversal flight approach into the framework of the AHA algorithm.
- Through comparative analysis, it has been shown that chaotic maps characterized by various invariant probability measures demonstrate significantly diverse optimization effects.
- An extensive set of numerical experiments has been conducted. Comparing CEAHA against 21 other meta-heuristic algorithms across CEC2014, CEC2019, and the most recent single objective benchmark test suite CEC2022, the experiments substantiate CEAHA's superior optimization capabilities.
- Through tests on 4 machine design problems, including pressure vessel, gear train, speed reducer, and piston lever, the superior practicability and robustness of CEAHA are verified.The rest of this paper is organized as follows. "Overview of artificial hummingbird algorithm" section presents a brief overview of the traditional artificial hummingbird algorithm. "Traversal efficiency of chaotic maps" section discusses the traversal efficiency of chaotic maps. "A novel enhanced artificial hummingbird algorithm" section proposes the structure of CEAHA. "Experimental results and discussion" section provides the experimental results, along with in-depth discussions and analyses of these outcomes. Finally, in the "Conclusions" section, a summary is provided, and potential directions for future research are pointed out.

Overview of artificial hummingbird algorithm
Given n food sources randomly, hummingbird population is randomly initialized:

$$x_i = Lb + rand(0,1) \cdot (Ub - Lb), i = 1, 2, \ldots, n \tag{1}$$

where Ub and Lb are the upper and lower boundaries, respectively. $rand(0.1)$ is a random vector in range $[0, 1]$, x_i represents the i-th candidate solution. Initialize the visit table for food sources as follows:

$$VT_{i,j} = \begin{cases} 0 & i \neq j \\ null & i = j \end{cases}, i = 1, 2, \ldots, n; j = 1, 2, \ldots, n \tag{2}$$

where for i = j, $VT_{i,j} = null$ signifies that the i-th hummingbird is feeding at its designated source; for $i \neq j$, $VT_{i,j} = 0$ denotes the i-th hummingbird's recent visit to the j-th food source in the current iteration.

The hummingbird's three flight skills (including axial flight, diagonal flight, and omnidirectional flight) are perfectly expressed, all with the help of the direction tangent vector. The specific expressions of hummingbird's flight skills in d-dimension (d-D) space are as follows:
   Axial flight:

$$D_{Af}^{(i)} = \begin{cases} 1 & i = randi([1,d]) \\ 0 & others \end{cases} \tag{3}$$

Diagonal flight:

$$D_{Df}^{(i)} = \begin{cases} 1 & i = P(i), j \in [1,k] \\ 0 & others \end{cases} \tag{4}$$

where,

$$P = randperm(k), k \in [2, \lceil r_1 \cdot (d-2) \rceil + 1] \tag{5}$$

Omnidirectional flight:

$$D_{Of}^{(i)} = 1, \ i = 1, \ldots, d \tag{6}$$

$randi([1, d])$ generates random integers from $[1, d]$, $randperm(k)$ produces a random permutation from 1 to k, r_1 is a random number within $(0, 1)$, and d signifies the spatial dimension of the target problem. Moreover, AHA emulates hummingbird foraging strategies: guided, territorial, and migratory.

Guided foraging:

$$v_i(t+1) = x_{i,tar}(t) + \alpha \cdot D_t \cdot (x_i(t) - x_{i,tar}(t)), \alpha \sim N(0,1) \tag{7}$$

Territorial foraging:

$$v_i(t+1) = x_i(t) + b \cdot D_t \cdot x_i(t), b \sim N(0,1) \tag{8}$$

where $x_i(t)$ represents the i-th hummingbird's position at time t, $x_{i,tar}(t)$ is the targeted source for the i-th hummingbird, and $\alpha \sim N(0,1)$ is a normally distributed guiding factor. $D_t \in \{D_{Af}, D_{Df}, D_{Of}\}$ indicates the flight skill employed: axial, diagonal, or omnidirectional.

When mod(t,2n)=0, the hummingbird with worst flight position update to new food source through migratory foraging:

$$x_{wor}(t+1) = Low + r \cdot (Up - Low) \tag{9}$$

where x_{wor} is the worst candidate solution.

The updating method for the hummingbird's position is as follows:

$$x_i(t+1) = \begin{cases} x_i(t) & f(x_i(t)) \leq f(v_i(t+1)) \\ v_i(t+1) & f(x_i(t)) > f(v_i(t+1)) \end{cases} \tag{10}$$

where $f(x_i(t))$ and $f(v_i(t+1))$ represent the fitness values of the candidate solution $x_i(t)$ and the updated solution $v_i(t+1)$, respectively. Although the unique flight skills and design of the visit table in AHA significantly enhance its optimization performance compared to earlier meta-heuristic algorithms, there are still some weaknesses. For example, as the iterations progress, the population diversity of AHA gradually declines, and its local exploitation ability weakens accordingly. This leads to a slow convergence rate, making it challenging to accurately find the optimal solution, and it may easily fall into the predicament of local optima.

Traversal efficiency of chaotic maps

While numerous studies have highlighted chaos as an effective method to improve the performance of meta-heuristic algorithms, how to integrate chaotic maps into algorithmic optimization design continues to be an area of active research. The statistical properties of chaotic maps are known to play a crucial role in influencing global search efficiency and computational effectiveness[61,71–73]. Detailed investigations into chaotic optimization[60,74–77] have considered the factors like the discreteness, probability density functions, and Lyapunov exponents of chaotic sequences, with particular attention to the Tent map's notable advantages in population initialization and global search. These findings are further supported by empirical results obtained from the chaotic accelerated particle swarm optimization[60], chaotic whale optimization algorithm[69] and chaotic dwarf mongoose optimization algorithm[64].

In order to further explore the internal mechanism of chaotic optimization, eight common chaotic maps are documented in Table 1, detailing their formulations, values of control parameters, experimental parameter values, and associated Lyapunov exponents (LEs). The positive LEs under the parameters listed in Table 1 indicate that these motion equations have all entered a state of chaotic behavior.

Consider the countable subset $C^n(x_0)$ produced by a chaotic map, as listed in Table 1, starting from any initial value x_0 within the chaotic regime X. And $\{C^n(x_0)\}$ forms a semi-flow on the measured space $(X, \mathcal{B}, \mu)$ if it adheres to the conditions: (1) the mapping $C^n : X \to X$, for $\forall n \in R^+$; (2) $C^{t+s} = C^t \circ C^s$, for $t, s \in R^+$, $x_0 \in X$; (3) the function: $C^n(x) : X \times R^+ \to X$ is continuous with respect to each n[82].

By a measure on X, any probability measure defined on the Borel σ-algebra $\mathcal{B}(X)$ subsets of X is referred. A measure μ is invariant under a transformation C, if $\mu(A) = \mu(C_t^{-1}(A))$ holds for each $t \in R^+$ and $\forall A \in \mathcal{B}$. Under the assumption that $(X, \mathcal{B}, \mu)$ is a σ-finite measure space, the Birkhoff Ergodic Theorem[83] assures that, for any function f in $L^1(\mu)$, the time average $\frac{1}{n}\sum_{i=0}^{n-1} f(C^i(x))$ a.e. converges to a function $f^* \in L^1(\mu)$

, if $C : (X, \mathcal{B}, \mu) \to (X, \mathcal{B}, \mu)$ is measure-preserving, where $L^1(X, \mathcal{B}, \mu)$ is a Banach space with the norm $||f||_1 = \int |f| d\mu$. Similarly, $\int f^* d\mu = \int_X X f d\mu$ is true, if a.e. $f^* \circ C = f^*$ and $\mu(x) < \infty$. Of course, when $C : (X, \mathcal{B}, \mu) \to (X, \mathcal{B}, \mu)$ exhibits ergodicity, The invariant measure f^* is almost everywhere constant and does not depend on the initial conditions of the chaotic maps. The invariant probability measure functions f^* of each chaotic map, which are scaled into the (0, 1) interval to facilitate comparison, are shown in Fig. 2. It is intuitive to see from Fig.2, these maps can be categorized into three types: those exhibiting uniform distribution characteristics (including Tent, Bernoulli, and piecewise linear chaotic map (PLCM)), which are shown in Fig. 2a; those with U-shaped distribution characteristics (including Logistic, Chebyshev and Cubic), which are shown in Fig. 2b; and those demonstrating Spike and Gaussian-like distributions (including 2D-NHM and Circle), which are shown in Fig. 2b.

The objective solution space X is assumed to be uniformly divided into N subintervals, where N represents the population size of the metaheuristic optimization algorithm. To achieve a point set $C^n(x_0)$ that perfectly fills these N subintervals, the ratio of the number of elements μ in set $C^n(x_0)$ to the number of subintervals N is defined as the traversal efficiency (TE) of the chaotic map. The "Perfect filling" refers to the condition where if $\mu(C^n(x_0))$ decreases by one, there is exactly one subinterval without any elements in $C^n(x_0)$. The lower the ratio, the higher the traversal efficiency, which can be expressed by the following mathematical formula:

Chaotic maps	Equations	Parameter value	LEs
Tent[72]	$x_{n+1} = \begin{cases} x_n/\gamma & 0 < x_n < \gamma \\ (1 - x_n)/(1 - \gamma) & \gamma < x_n < 1 \end{cases}$	$\gamma = 0.4$	3.6247
Bernoulli[73]	$x_{n+1} = \begin{cases} x_n/(1 - \lambda) & 0 < x_n < 1 - \lambda \\ (x_n - (1 - \lambda))/\lambda & 1 - \lambda < x_n < 1 \end{cases}$	$\lambda = 0.4$	8.0583
PLCM[78]	$x_{n+1} = \begin{cases} x_n/p & 0 \le x_n < p \\ (x_n - p)/(0.5 - p) & p \le x_n < 1/2 \\ (1 - p - x_n)/(0.5 - p) & 1/2 \le x_n < 1 - p \\ (1 - x_n)/p & 1 - p \le x_n < 1 \end{cases}$	$p = 0.4$	4.2644
2D-NHM[79]	$\begin{cases} x_{n+1} = \beta \sin(\sigma x_n)\sin(\mu/y_n) \\ y_{n+1} = x_n \end{cases}$	$\beta = 2, \sigma = \pi, \mu = 11$	2.1167, 1.1850
Circle[80]	$x_{n+1} = \mathrm{mod}(x_n + \Omega - (K/2\pi)\sin(2\pi x_n), 1)$	$\Omega = 0.5, K = 2.2$	0.5766
Logistic[81]	$x_{n+1} = \mu x_n(1 - x_n)$	$\mu = 4$	0.6934
Chebyshev[76]	$x_{n+1} = \cos(k\cos^{-1} x_n)$	$k = 5$	1.6101
Cubic[77]	$x_{n+1} = \lambda x_n^3 + (1 - \lambda)x_n$	$\lambda = 4$	1.5827

Table 1. Equations of chaotic maps.

(a) Uniform distribution   **(b)** U-shaped distribution   **(c)** Spike and Gaussian-like distributions
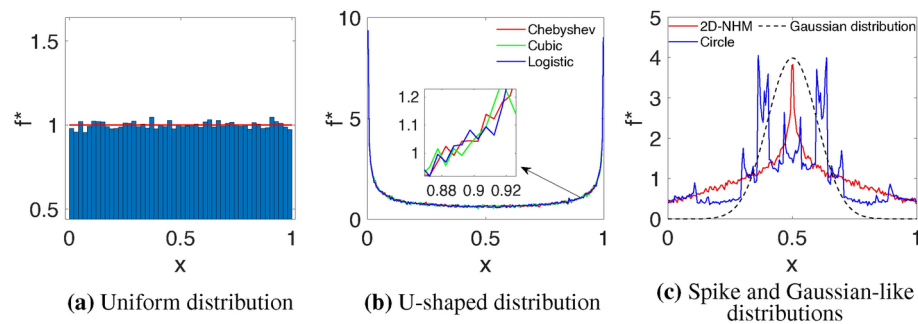
Figure 2. Analysis of invariant probability measure functions f^* for 8 chaotic maps.
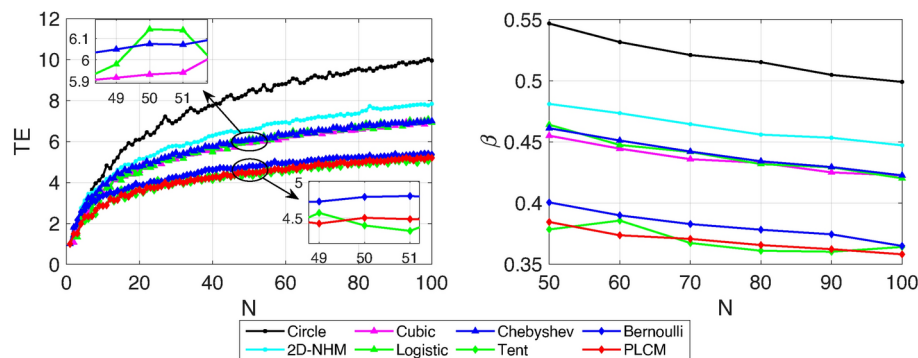

Figure 3. Comparison curves of the TE and β for 8 chaotic maps across different values of the population size N.

$$TE = \frac{1}{k} \sum_{i=1}^{k} \frac{\mu(C^n(x_0))}{N} \tag{11}$$

where k represents the average value taken over multiple experimental results.

As illustrated in the left image of Fig. 3, the comparison curves of the traversal efficiency for eight chaotic maps in Table 1 across different values of N demonstrate that the chaotic maps with an invariant probability measure of $f^* = 1$ (i.e., PLCM, Bernoulli, and Tent maps) exhibit the highest efficiency in traversing space. The U-shaped distribution maps like Chebyshev, Logistic, and Cubic follow, while the 2D-NHM and Circle maps show relatively lower traversal efficiency. Therefore, using chaotic maps with $f^* = 1$ for population initialization is the optimal choice to lay the groundwork for subsequent spatial exploration by intelligent agents. Moreover, the left image of Fig. 3 reveals that the traversal efficiency curves conform to a power-law distribution $TE \in N^{\beta}$, allowing the expression of the traversal efficiency exponent β ($0 < \beta < 1$) to be represented as:

$$\beta = \lim_{N \to \infty} \log_N(TE) = \lim_{N \to \infty} \left(\log_N \left(\sum_{i=1}^{k} \mu(C^n(x_0)) \right) - \log_N k - 1 \right) \tag{12}$$

Under the definition of the measure β, the traversal efficiency becomes an inherent feature of the chaotic map. The right image of Fig. 3 shows the calculated values of β for various chaotic maps, which reveal that the exponent β exhibits the same three patterns as TE; specifically, chaotic maps with an invariant probability measure of $f^* = 1$ offer optimal traversal in the solution space. And although the Tent, PLCM, and Bernoulli all have an f^* value of 1, there are still slight differences in their values of TE and β. For instance, with a population size of $N = 50$, the TE for Tent is better than PLCM and surpasses Bernoulli (see Fig. 3). And an in-depth analysis of the optimization effects that these three types of chaotic systems have on algorithm performance is conducted in the "Efficiency of CEAHA with different chaotic maps" section.

A novel enhanced artificial hummingbird algorithm

In order to further improve the performance of AHA, a novel enhanced artificial hummingbird algorithm with chaotic traversal flight (CEAHA) is proposed. Given that the experiments in this paper are set with a population size of 50 and and taking into account the conclusions of Section, Section will employ the Tent map

for population initialization and migratory foraging, laying the groundwork for iterative updates and exploration of the solution space in the algorithm.

Require: $N, d, f(x), X_i, T_{max}, Lb, Ub$, chaotic equations.
Ensure: Output optimal results
1: Initialize positions x_i of N hummingbirds using d-dimensional chaotic vectors $T^t(i,d)$, and set up the visitation record (Visit_table) and fitness values for each hummingbird x_i: the previous $f_{pre}(x_i)$ and current $f_{cur}(x_i)$.
2: Set $y_i = f(x_i)$, $y_g = \min(y_i)$, find the best global position P_g. Chaotic guiding coefficients c_1, c_2 generated by Tent map.
3: **while** $t \leq T_{max}$ **do**
4:     **for** ith hummingbird from 1 to n **do**
5:         **if** $c_1 < 1/3$ **then**
6:             Axial flight (Eq.3)
7:         **else if** $c_1 > 2/3$ **then**
8:             Diagonal flight (Eq.4)
9:         **else**
10:            Omnidirectional flight (Eq.5)
11:         **end if**
12:         **if** $c_2 \leq c_1$ **then**
13:             Guided foraging (Eq.7)
14:             Update the visit table and the position of individuals (Eq.10)
15:         **else**
16:             Territorial foraging (Eq.8)
17:             Update the visit table and the position of individuals (Eq.10)
18:         **end if**
19:         **if** $f_{cur}(x_i) - f_{pre}(x_i) == 0$ **then**
20:             Chaotic traversal flight (Eq.15)
21:             **if** $f(v_i(t+1)) < f(x_i(t))$ **then**
22:                 $x_i(t+1) = h_i(t+1)$
23:                 **for** jth food source from 1 to n **do**
24:                     Visit_table(j,i)
25:                     $= \max_{l \in n, l \neq j}$ (Visit_table(j,l))+1
26:                 **end for**
27:             **else**
28:                 **for** jth food source from 1 to n ($j \neq i$) **do**
29:                     Visit_table(i,j)=Visit_table(i,j)+1,
30:                 **end for**
31:             **end if**
32:         **end if**
33:         $f_{pre}(x_i)=f_{cur}(x_i)$.
34:     **end for**
35:     **if** mod($t,2N$)==0 **then** Chaotic migration foraging (Eq.14)
36:         Update the visit table and the position of individuals (Eq.16)
37:     **end if**
38: **end while**

Algorithm 1. Pseudo-code of CEAHA

The equation of Tent map is shown in the first row of Table 1. Place N hummingbird population on N food sources and use chaos numbers $T^t(i,d) \in \{C^t(x_0)\}$ generated by Tent map to initialize the population, as shown in the equation below:

$$x_i = Lb + T^t(i,d) \cdot (Ub - Lb) \tag{13}$$

where $T^t(i,d)$ denotes the d-dimensional chaotic vector generated by the i-th hummingbird at time t within the d-dimensional solution space.

During the migratory foraging process of hummingbirds, a chaos mechanism for global mutation is introduced to update the position of the individuals ranked last. This behavior prevents the worst individuals from lingering long on scarce and sterile food sources, and aids in the implementation of a chaotic traversal search throughout the global space. The expression of migratory foraging based on Tent map is presented in Eq. (14).

$$x_{wor}(t+1) = Lb + T^t(i,d) \cdot (Ub - Lb) \tag{14}$$

To reduce the overlapping movement of individuals and enhance search efficiency in algorithm, the chaotic traversal flight strategy leverages chaotic motion's ergodicity and non-repetitive properties for thoroughly exploiting local solution spaces. consider a population of N hummingbirds uniformly distributed across the solution space, where each bird has a unique spatial flight domain defined by $(Ub - Lb)/(N - 2 + 2 \cdot rand)$. The equation for chaotic domain traversal flight behavior, which is based on the chaotic map, can be formulated as follows:
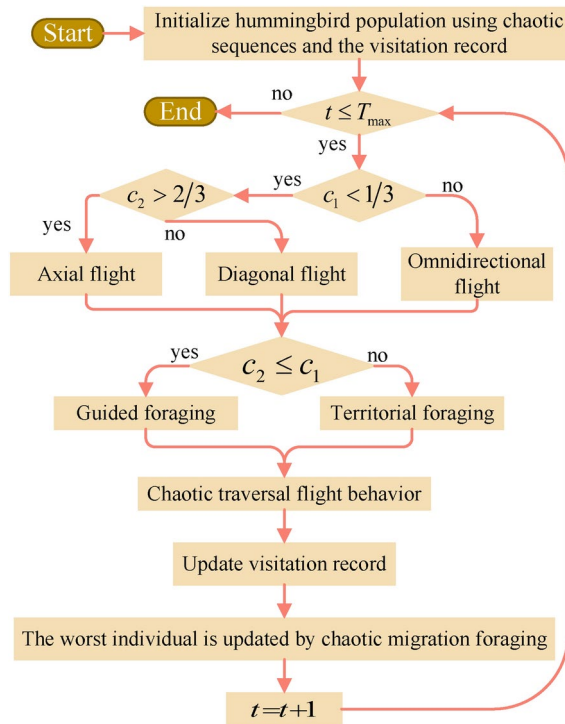
Figure 4. The workflow diagram of the proposed CEAHA.

Name	Formulations	Search ranges	D	values
Sphere	$F_1(x) = \sum\limits_{i=1}^{n} x_i^2$	$[-100, 100]$	30	0
Schwefel 2.22	$F_2(x) = \sum\limits_{i=1}^{n} |x_i| + \prod\limits_{i=1}^{n} |x_i|$	$[-10, 10]$	30	0
Schwefel 1.2	$F_3(x) = \sum\limits_{i=1}^{n} \left(\sum\limits_{j=1}^{i} x_j \right)^2$	$[-100, 100]$	30	0
Schwefel 2.21	$F_4(x) = \max\{|x_i|, 1 \leq i \leq n\}$	[-30,30]	30	0
Rosenbrock	$F_5(x) = \sum\limits_{i=1}^{n-1} \left(100(x_{i+1} - x_i)^2 \right) + (x_i - 1)^2$	$[-30, 30]$	30	0
Step	$F_6(x) = \sum\limits_{i=1}^{n} \left(\lfloor x_i + 0.5 \rfloor \right)^2$	$[-100, 100]$	30	0

Table 2. Unimodal benchmark functions used in the algorithm performance test experiments.

$$v_i(t+1) = H_i(t, d) \cdot (Ub - Lb)/(N - 2 + 2 * rand) \cdot D_t \cdot x_i(t) + x_i(t) \tag{15}$$

where $D_t \in \{D_{Af}, D_{Df}, D_{Of}\}$, and $H_i(t, d)$ represents the d-dimensional chaotic vector produced by the i-th hummingbird at time t within the d-dimensional solution space, following the equation in Table 1. To determine the most apt chaotic system from Table 1 for chaotic traversal flight, this work will assess and contrast the efficacy of various CEAHA algorithm incarnations with integrated chaotic maps in "Efficiency of CEAHA with different chaotic maps".

During chaotic traversal flights, candidate solutions identified are logged in a visit table and updated accordingly according to Eq. (10). If a hummingbird discovers a superior solution, its corresponding visit table entry is promptly upgraded to the highest level, directing the next phase of the population's guided foraging toward these high-value locations. Conversely, if the i-th hummingbird fails to find an improved solution post-chaotic traversal, the visit levels for the rest of the agents increase by 1, refocusing efforts on unexplored areas and reducing the likelihood of getting trapped in local optima. Therefore, the memory and search capabilities of the

Name	Formulations	Search ranges	D	values
Quartic	$F_7(x) = \sum\limits_{i=1}^{n} i \cdot x_i^2 + random[0,1)$	$[-1.28, 1.28]$	30	0
Schwefel	$F_8(x) = -\sum\limits_{i=1}^{n}(x_i \sin(\sqrt{|x_i|}))$	$[-500, 500]$	30	$-418.9829 \times D$
Rastrigin	$F_9(x) = -\sum\limits_{i=1}^{n}[x_i^2 - 10\cos(2\pi x_i) + 10]$	$[-5.12, 5.12]$	30	0
Ackley	$F_{10}(x) = -20\exp(-0.2\sqrt{\frac{1}{n}\sum\limits_{i=1}^{n}x_i^2})$ $-\exp(\frac{1}{n}\sum\limits_{i=1}^{n}\cos 2\pi x_i) + 20 + e$	$[-32, 32]$	30	0
Griewank	$F_{11}(x) = \frac{1}{400}\sum_{i=1}^{n}x_i^2 - \prod_{i=1}^{n}\cos(\frac{x_i}{\sqrt{i}}) + 1$	$[-600,600]$	30	0
Penalized	$F_{12}(x) = \frac{\pi}{n}\cdot 10\sin^2(3\pi y_1) + \frac{\pi}{n}\cdot\sum\limits_{i=1}^{n-1}(y_i - 1)^2\cdot[1 + 10\sin^2(\pi y_i + 1)] + \frac{\pi}{n}$ $\cdot(y_n - 1)^2 + \sum\limits_{i=1}^{30}u(x_i, 10, 100, 4)$	$[-50, 50]$	30	0
Penalized2	$F_{13}(x) = 0.1\sin^2(3\pi x_1) + 0.1\sum\limits_{i=1}^{29}(x_i - 1)^2$ $\cdot p\cdot[1 + \sin^2(3\pi x_{i+1})] + 0.1(x_n - 1)^2[1 + \sin^2(2\pi x_{30})] + \sum\limits_{i=1}^{30}u(x_i, 5, 100, 4)$	$[-50, 50]$	30	0

Table 3. Multimodal benchmark functions used in the algorithm performance test experiments.

Name	Formulations	Search ranges	D	values
Foxholes	$F_{14}(x) = [\frac{1}{500} + \sum\limits_{j=1}^{25}\frac{1}{j + \sum\limits_{j=1}^{2}(x_i - a_{ij})^6}]^{-1}$	$[-65.536, 65.536]$	2	0.998
Kowalik	$F_{15}(x) = \sum\limits_{i=1}^{11}\left|a_i - \frac{x_1(b_i^2 + b_i x_2)}{b_i^2 + b_i x_3 + x_4}\right|^2$	$[-5, 5]$	4	0.00031
Six Hump Camel Back	$F_{16}(x) = 4x_1^2 - 2.1x_1^4 + \frac{1}{3}x_1^6 + x_1 x_2 - 4x_2^2 + 4x_2^4$	$[-5, 5]$	2	-1.03163
Branin	$F_{17}(x) = (x_2 - \frac{5.1}{4\pi^2}x_1^2 + \frac{5}{\pi}(x_1 - 6)^2 + 10(1 - \frac{1}{8\pi}))\cos(x_1) + 10$	$[-5,5]$	2	0.398
GoldStein-Price	$F_{18}(x) = [1 + (x_1 + x_2 + 1)^2(19 - 14x_1 + 3x_1^2 - 14x_2 + 6x_1 x_2 + 3x_2^2)]$ $\cdot[30 + (2x_1 + 1 - 3x_2)^2(18 - 32x_1 + 12x_1^2 + 48x_2 - 36x_1 x_2 + 27x_2^2)]$	$[-2, 2]$	2	3
Hartman3	$F_{19}(x) = -\sum\limits_{i=1}^{4}\exp\left[-\sum\limits_{j=1}^{3}a_{ij}(x_j - p_{ij})^2\right]$	$[0, 1]$	3	-3.86
Hartman6	$F_{20}(x) = -\sum\limits_{i=1}^{4}\exp\left[-\sum\limits_{j=1}^{6}a_{ij}(x_j - p_{ij})^2\right]$	$[0, 1]$	6	-3.32
Shekel5	$F_{21}(x) = -\sum\limits_{i=1}^{5}\left|(x_i - a_i)(x_i - a_i)^T + c_i\right|^{-1}$	$[0, 10]$	4	-10.1532
Shekel7	$F_{22}(x) = -\sum\limits_{i=1}^{7}\left|(x_i - a_i)(x_i - a_i)^T + c_i\right|^{-1}$	$[0, 10]$	4	-10.4028
Shekel10	$F_{23}(x) = -\sum\limits_{i=1}^{10}\left|(x_i - a_i)(x_i - a_i)^T + c_i\right|^{-1}$	$[0, 10]$	4	-10.5363

Table 4. Fixed-dimension multimodal benchmark functions used in the algorithm performance test experiments.

Figure 5. Comparative images (F1–F8) of the average convergence and diversity curves of 8 CEAHA variants with distinct chaotic maps versus the original AHA. Left 1 and 2 are the 3D plots and 2D contour maps of the test function, respectively, with a red asterisk (*) indicating the optimal solution. Left 3 and 4 illustrate the average convergence and diversity curves, respectively.
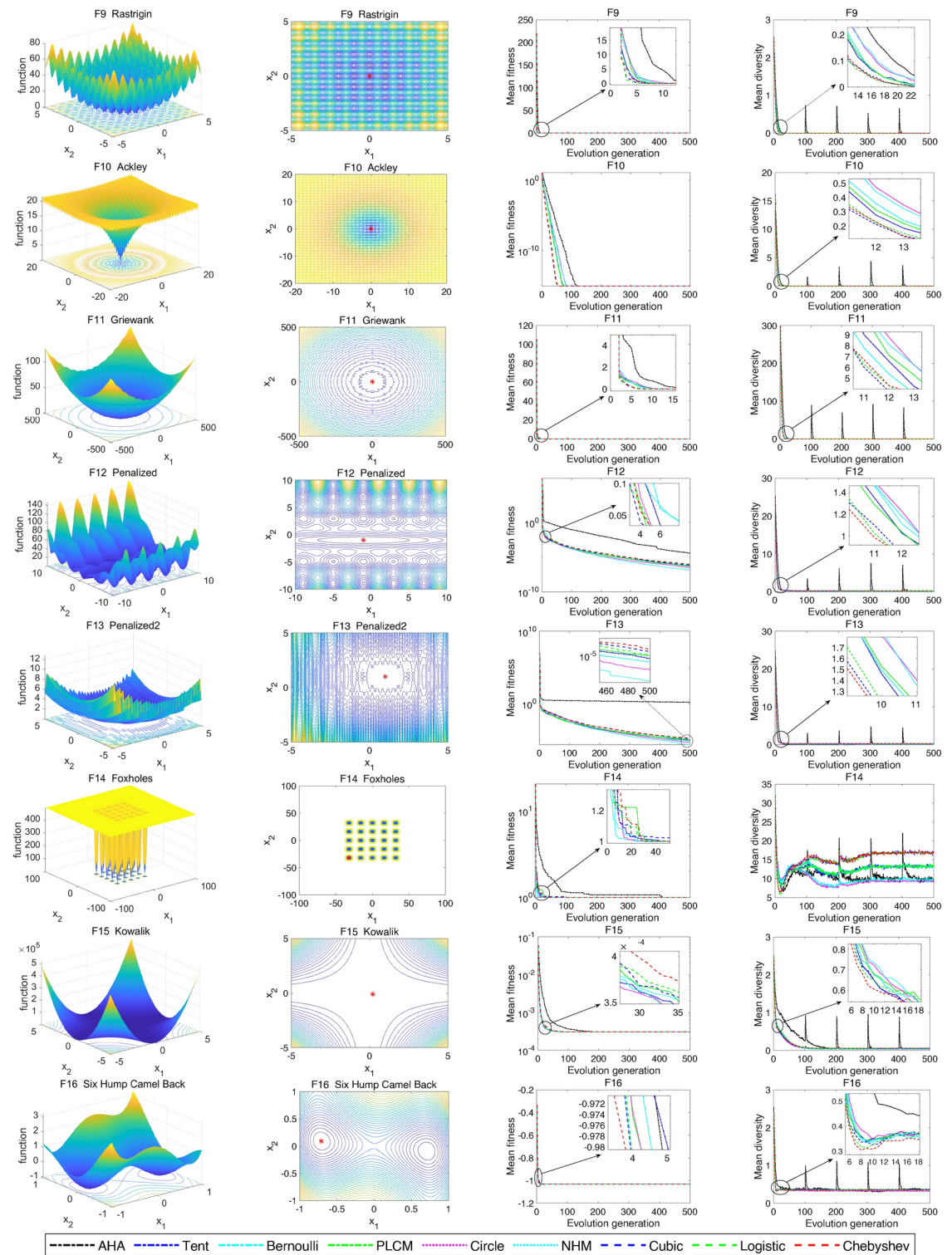
Figure 6. Comparative images (F9–F16) of the average convergence and diversity curves of 8 CEAHA variants with distinct chaotic maps versus the original AHA. Left 1 and 2 are the 3D plots and 2D contour maps of the test function, respectively, with a red asterisk (*) indicating the optimal solution. Left 3 and 4 illustrate the average convergence and diversity curves, respectively.
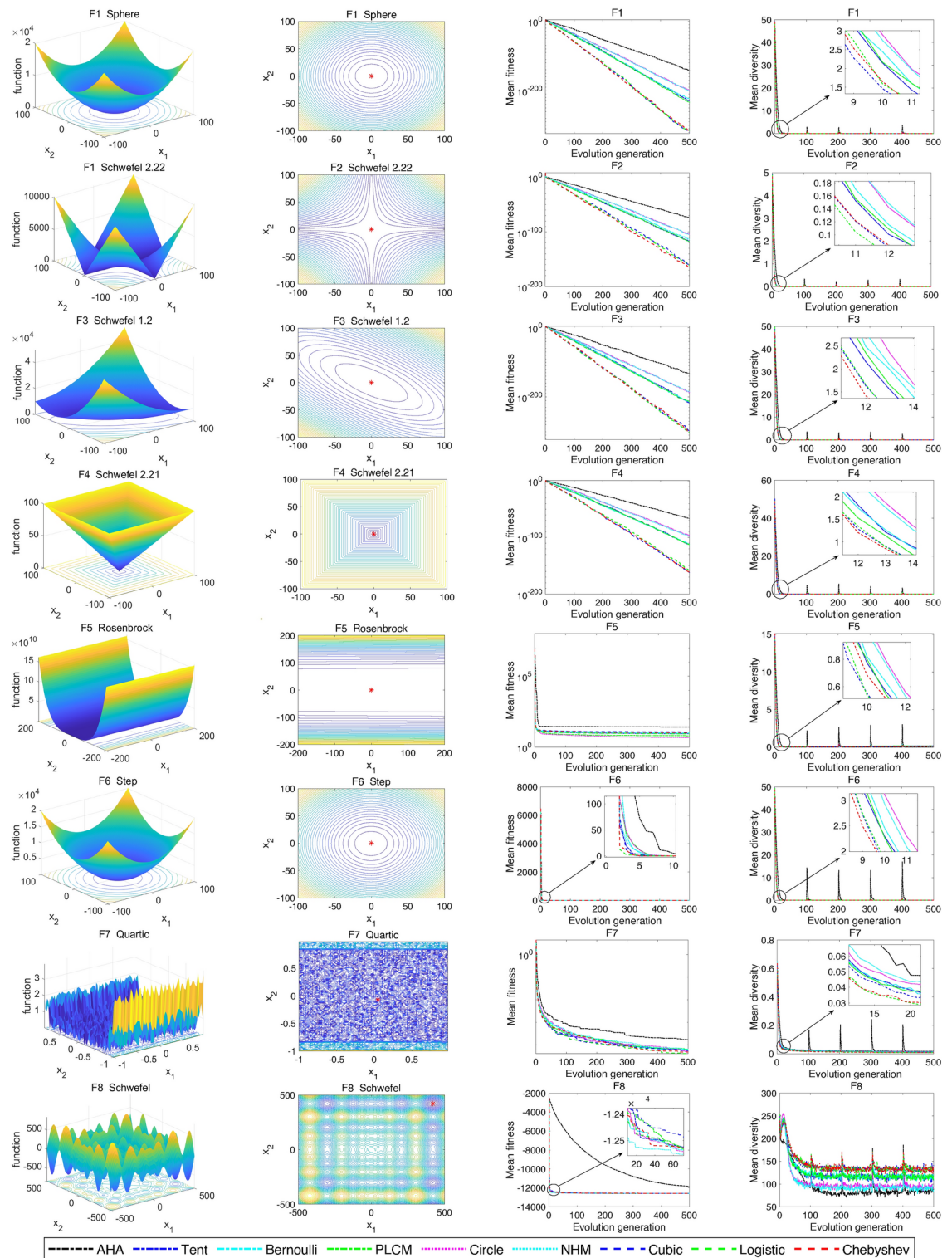
Figure 7. Comparative images (F17–F23) of the average convergence and diversity curves of 8 CEAHA variants with distinct chaotic maps versus the original AHA. Left 1 and 2 are the 3D plots and 2D contour maps of the test function, respectively, with a red asterisk (*) indicating the optimal solution. Left 3 and 4 illustrate the average convergence and diversity curves, respectively.
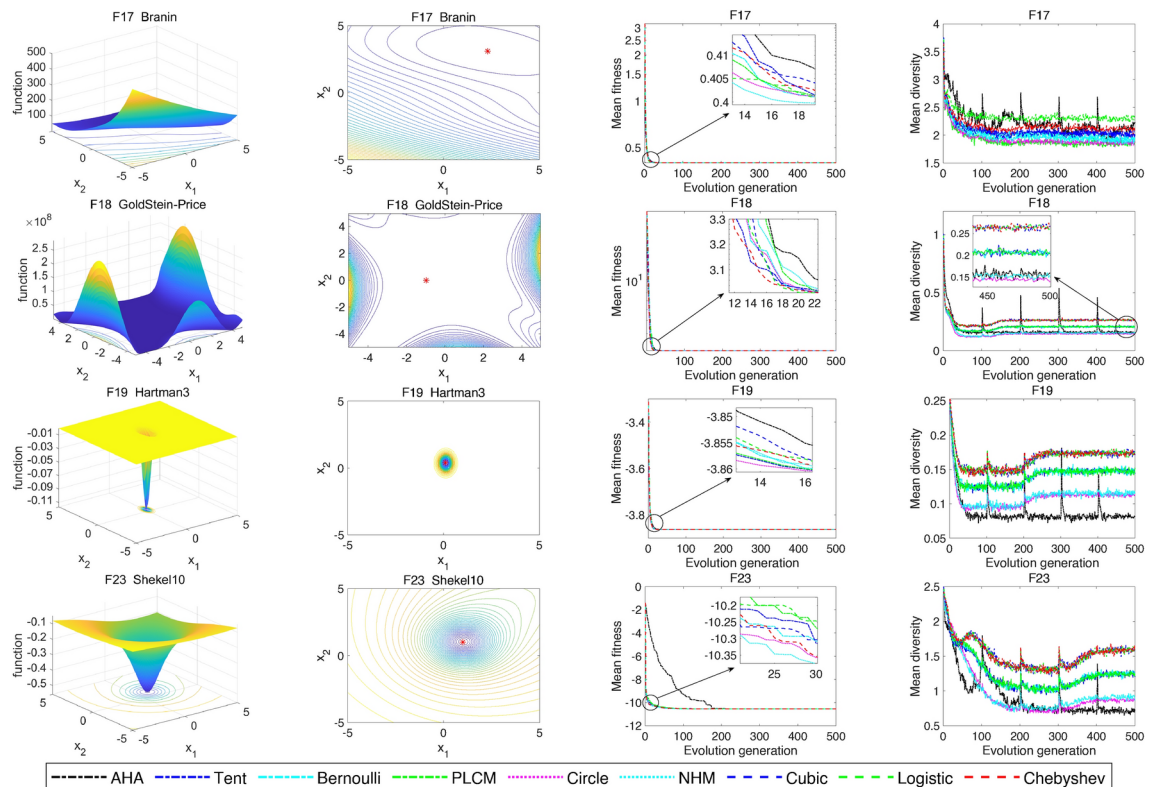
hummingbirds are expanded, ensuring a comprehensive examination of available food sources. The pseudo-code and algorithmic workflow diagram of the proposed CEAHA are illustrated in Algorithm 1 and Fig. 4.

In Algorithm 1, $f_{cur}(x_i)$ and $f_{pre}(x_i)$ denote the visit levels of a hummingbird at the current and previous moments, respectively. As shown in Eq. (16), if the visit level at a hummingbird's location remains unchanged, (i.e., $f_{cur}(x_i) - f_{pre}(x) = 0$), indicating a loss of activity, chaotic traversal flight behavior is initiated to enhance diversity and facilitate precise exploitation of nearby optimal solutions.

$$x_i(t+1) = \begin{cases} v_i(t+1) & if \quad f_{cur}(x_i) - f_{pre}(x) = 0 \\ x_i(t) & others \end{cases} \tag{16}$$

Experimental results and discussion

To rigorously evaluate the optimization performance of the eight chaotic maps in Table 1 and the efficacy of the CEAHA, this study devises two sets of experiments. The first experiment is designed to investigate the performance variations when integrating 8 different chaotic maps into the CEAHA algorithm, using a comprehensive assessment with 23 standard test functions[42]. These 23 functions included unimodal (F1–F7), multimodal (F8–F13), and fixed-dimension multimodal functions (F14–F23), with their formulas and expressions presented in Table 2, 3 and 4. Moreover, this part delves into the inherent mechanics of chaotic search, considering the ergodicity of chaotic sequences and their effects on population diversity.

In the second experiment, the best-performing variant of CEAHA from the first set is benchmarked against 21 popular meta-heuristic algorithms (see Table 6, where the parameter values for each algorithm are extracted from the respective original publications) on the recent single-objective optimization test suite CEC2022[84], and supplemented with additional benchmarks on CEC2014[43] and CEC2019[85] suites due to CEC2022's category limitations.

To ensure fairness, all algorithms in this study are configured with a population size of 50 and a maximum iteration count of 500 ($T_{max} = 500$). Each algorithm is run independently 30 times to evaluate average convergence and robustness. And the maximum number of fitness evaluation for each algorithm is 25000. The hardware configuration of the computer used in this study is an AMD Ryzen 7-5800H CPU with Radeon Graphics @ 3.20 GHz, and the simulation platform used for implementing all the algorithms and comparative experiments mentioned in this paper is MATLAB R2021b. Detailed experimental procedures and analysis are elaborated in the following sections.

Fun	Index	AHA-Cubic	AHA	AHA-Tent	AHA-Bernoulli	AHA-PLCM	AHA-Logistic	AHA-Chebyshev	AHA-2D-NHM	AHA-Circle
F1	Mean	4.66E−321	1.50E−138+	4.41E−232≈	7.35E−227+	2.91E−232+	5.43E−322≈	2.77E−321≈	6.26E−207+	2.17E−203+
	Std	0.00E+00	8.22E−138	0.00E+00	0.00E+00	0.00E+00	0.00E+00	0.00E+00	0.00E+00	0.00E+00
F2	Mean	5.83E−163	1.20E−76+	9.94E−119+	2.93E−119+	7.77E−119+	1.31E−161≈	5.55E−165≈	6.76E−105+	9.58E−104+
	Std	3.14E−162	3.22E−76	5.23E−118	1.53E−118	3.69E−118	7.20E−161	0.00E+00	3.69E−104	4.44E−103
F3	Mean	1.69E−303	4.83E−131+	4.28E−221+	1.16E−215+	5.65E−214+	1.55E−293≈	1.38E−305≈	4.73E−191+	9.14E−185+
	Std	0.00E+00	2.63E−130	0.00E+00	0.00E+00	0.00E+00	0.00E+00	0.00E+00	0.00E+00	0.00E+00
F4	Mean	7.57E−158	1.03E−66+	1.25E−111+	1.44E−113+	5.03E−114+	9.63E−154≈	7.94E−161≈	3.81E−100+	3.75E−97+
	Std	4.14E−157	3.41E−66	6.85E−111	4.44E−113	1.96E−113	5.27E−153	4.29E−160	1.31E−99	1.93E−96
F5	Mean	1.18E+01	2.63E+01+	8.93E+00≈	1.10E+01≈	6.43E+00≈	8.75E+00≈	1.04E+01≈	9.43E+00-	4.78E+00-
	Std	1.24E+01	4.17E−01	1.19E+01	1.23E+01	1.07E+01	1.21E+01	1.20E+01	1.22E+01	9.48E+00
F6	Mean	0.00E+00	0.00E+00≈	0.00E+00≈	0.00E+00≈	0.00E+00≈	0.00E+00≈	0.00E+00≈	0.00E+00≈	0.00E+00≈
	Std	0.00E+00	0.00E+00	0.00E+00	0.00E+00	0.00E+00	0.00E+00	0.00E+00	0.00E+00	0.00E+00
F7	Mean	4.11E−05	1.63E−04+	6.91E−05≈	6.68E−05+	6.88E−05+	4.50E−05≈	4.62E−05≈	6.48E−05+	8.61E−05+
	Std	3.97E−05	1.27E−04	6.61E−05	4.78E−05	4.69E−05	3.09E−05	3.65E−05	4.60E−05	6.85E−05
F8	Mean	− 1.26E+04	-1.18E+04+	− 1.26E+04-	− 1.26E+04-	− 1.26E+04≈	− 1.26E+04≈	− 1.26E+04≈	− 1.26E+04-	− 1.26E+04-
	Std	2.63E−01	3.69E+02	1.60E−01	1.07E−01	2.17E−01	1.71E−01	1.56E−01	5.85E−02	1.38E−01
F9	Mean	0.00E+00	0.00E+00≈	0.00E+00≈	0.00E+00≈	0.00E+00≈	0.00E+00≈	0.00E+00≈	0.00E+00≈	0.00E+00≈
	Std	0.00E+00	0.00E+00	0.00E+00	0.00E+00	0.00E+00	0.00E+00	0.00E+00	0.00E+00	0.00E+00
F10	Mean	8.88E−16	8.88E−16≈	8.88E−16≈	8.88E−16≈	8.88E−16≈	8.88E−16≈	8.88E−16≈	8.88E−16≈	8.88E−16≈
	Std	0.00E+00	0.00E+00	0.00E+00	0.00E+00	0.00E+00	0.00E+00	0.00E+00	0.00E+00	0.00E+00
F11	Mean	0.00E+00	0.00E+00≈	0.00E+00≈	0.00E+00≈	0.00E+00≈	0.00E+00≈	0.00E+00≈	0.00E+00≈	0.00E+00≈
	Std	0.00E+00	0.00E+00	0.00E+00	0.00E+00	0.00E+00	0.00E+00	0.00E+00	0.00E+00	0.00E+00
F12	Mean	7.05E−07	3.46E−05+	4.47E−07	6.26E−07≈	3.76E−07-	9.59E−07≈	9.28E−07≈	1.74E−07	2.85E−07
	Std	5.24E−07	3.51E−05	4.86E−07	5.15E−07	2.75E−07	6.24E−07	7.53E−07	2.09E−07	1.91E−07
F13	Mean	1.15E−05	1.74E+00+	7.97E−06≈	7.10E−06-	7.47E−06≈	1.03E−05≈	9.54E−06≈	1.98E−06-	4.37E−06-
	Std	9.41E−06	5.65E−01	7.06E−06	6.19E−06	6.93E−06	8.41E−06	5.86E−06	1.86E−06	3.54E−06
F14	Mean	9.98E−01	1.06E+00≈	9.98E−01≈	9.98E−01≈	9.98E−01≈	9.98E−01≈	9.98E−01≈	9.98E−01≈	9.98E−01≈
	Std	0.00E+00	3.62E−01	0.00E+00	0.00E+00	0.00E+00	0.00E+00	0.00E+00	0.00E+00	0.00E+00
F15	Mean	3.07E−04	3.07E−04+	3.07E−04≈	3.07E−04≈	3.07E−04≈	3.07E−04≈	3.07E−04≈	3.07E−04≈	3.07E−04≈
	Std	5.77E−16	3.58E−15	9.75E−17	6.12E−16	7.79E−18	6.46E−18	3.37E−18	4.88E−18	1.83E−17
F16	Mean	-1.03E+00	-1.03E+00≈	-1.03E+00≈	-1.03E+00≈	-1.03E+00≈	-1.03E+00≈	-1.03E+00≈	-1.03E+00-	-1.03E+00≈
	Std	6.12E−16	6.05E−16	5.83E−16	6.05E−16	5.83E−16	5.76E−16	5.90E−16	5.53E−16	5.76E−16
F17	Mean	3.98E−01	3.98E−01≈	3.98E−01≈	3.98E−01≈	3.98E−01≈	3.98E−01≈	3.98E−01≈	3.98E−01≈	3.98E−01≈
	Std	0.00E+00	0.00E+00	0.00E+00	0.00E+00	0.00E+00	1.59E−13	0.00E+00	0.00E+00	0.00E+00
F18	Mean	3.00E+00	3.00E+00≈	3.00E+00≈	3.00E+00≈	3.00E+00≈	3.00E+00≈	3.00E+00≈	3.00E+00≈	3.00E+00≈
	Std	1.27E−15	1.34E−15	1.25E−15	1.26E−15	1.25E−15	2.16E−15	1.28E−15	1.29E−15	1.33E−15
F19	Mean	-3.86E+00	-3.86E+00≈	-3.86E+00≈	-3.86E+00≈	-3.86E+00≈	-3.86E+00≈	-3.86E+00≈	-3.86E+00≈	-3.86E+00≈
	Std	2.71E−15	2.71E−15	2.71E−15	2.71E−15	2.71E−15	2.71E−15	2.71E−15	2.71E−15	2.71E−15
F20	Mean	-3.32E+00	-3.32E+00≈	-3.32E+00≈	-3.32E+00≈	-3.32E+00≈	-3.32E+00≈	-3.32E+00≈	-3.32E+00≈	-3.32E+00≈
	Std	1.36E− 15	2.17E− 02	1.36E− 15	1.36E− 15	1.34E− 15	1.36E− 15	1.34E− 15	1.36E− 15	1.34E− 15
F21	Mean	-1.02E+01	− 1.02E+01≈	-1.02E+01≈	-1.02E+01≈	-1.02E+01≈	− 1.02E+01≈	− 1.02E+01≈	-1.02E+01≈	-1.02E+01≈
	Std	6.33E−15	1.35E−05	6.51E−15	6.14E−15	6.51E−15	6.39E−15	6.33E−15	6.68E−15	6.51E−15
F22	Mean	− 1.04E+01	-1.04E+01≈	-1.04E+01≈	− 1.04E+01≈	− 1.04E+01	− 1.04E+01≈	− 1.04E+01≈	− 1.04E+01≈	− 1.04E+01≈
	Std	0.00E+00	2.70E−11	3.30E−16	4.66E−16	8.73E−16	3.30E−16	5.71E−16	4.66E−16	4.66E−16
F23	Mean	− 1.05E+01	− 1.05E+01≈	− 1.05E+01≈	− 1.05E+01≈	− 1.05E+01≈	− 1.05E+01≈	− 1.05E+01≈	-1.05E+01≈	-1.05E+01≈
	Std	2.62E−15	3.92E−15	1.23E−15	2.49E−15	9.33E−16	1.04E−15	1.14E−15	2.62E−15	1.14E−15
Cubic wins	+	10	4	5	5	0	0	5	5	
Similar	≈	13	17	16	16	23	23	13	14	
Other wins	−	0	2	2	2	0	0	5	4	

Table 5. Statistical results of eight CEAHA versions with eight different chaotic maps on 23 test functions.

Efficiency of CEAHA with different chaotic maps

Figures 5, 6, and 7 present the average convergence and average population diversity curves for the eight versions of CEAHA compared with the original AHA, after 30 independent runs on 23 standard benchmark functions. Diversity is defined as the distance between solutions or clusters of solutions within the search space[86]. To

Algorithms	Parameters
CEAHA	Migration coefficient $M = 2n$
Artificial hummingbird algorithm (AHA)[43]	Migration coefficient $M = 2n$
Artificial hummingbird algorithm based on golden sine factor (DGSAHA)[67]	Crossover probability $P_{CR} = 0.13$; Mutation scaling factor $L = 0.2$; golden sine factor $\alpha = \pi, \beta = -\pi, h = (\sqrt{5} - 1)/2$
Improved artificial hummingbird algorithm (IAHA)[68]	Lévy flight coefficient $\beta = 1.5, \alpha = 0.01$; Parameter of Chebyshev map $k = 4$
Multi-strategy boosted hybrid artificial hummingbird algorithm (LCAHA)[47]	Lévy flight coefficient $\beta = 1.5, \alpha = 0.01$
Electric eel foraging optimization (EEFO)[37]	Energy factor $E_0 = 4sin(1 - t/T), E = ln(1/rand)$;
	scale of resting area $\alpha = 2(e - e^{t/T}) \cdot \sin(2\pi \cdot rand)$
	scale of hunting area $\beta = 2(e - e^{t/T}) \cdot \sin(2\pi \cdot rand)$;
	Curling factor $\varepsilon = e^{rand \cdot (1-t)/T} \cdot \cos(2\pi \cdot rand)$
Evolutionary mating algorithm (EMA)[13]	Crossover probability $C_r = 0.8$; Probability of encountering the predator $r = 0.2$
Grasshopper optimization algorithm (GOA)[39]	Adaptive parameter $(c_{\min} = 0.00004, c_{\max} = 1)$; intensity of attraction $f = 0.5$; attractive length scale $l = 1.5$
Sinh cosh optimizer (SCHO)[26]	$u = 0.388, m = 0.45, n = 0.5, p = 10$, $q = 9, \alpha = 4.6, \beta = 1.55, ct = 3.6$, $BS = floor(T/\beta), T = floor(T/ct), BSi = 0, BSi_{temp} = 0$
Student psychology based optimization (SPBO)[32]	Proportions of second-best students, general students, and students to be promoted are 5/15, 8/15, 2/15, respectively.
Whale optimization algorithm (WOA)[36]	$\overrightarrow{A} = 2\overrightarrow{a} \cdot \overrightarrow{r} - \overrightarrow{a}; \overrightarrow{C} = 2 \cdot \overrightarrow{r}; \overrightarrow{a} \in [0, 2]; \overrightarrow{r} \in [0, 1]$
Particle swarm optimization (PSO)[35]	Cognitive coefficient is 2; social coefficient is 2; inertia constant is 0.8
Cuckoo search algorithm (CS)[87]	Mutation probability is 0.25
Arithmetic optimization algorithm (AOA)[88]	Range of acceleration function [0.2, 1], control parameter 0.499, sensitive parameter 5
Salp swarm algorithm (SSA)[40]	Control parameters $r_1 = 2e^{-(\frac{4l}{L})^2}, r_2 \in [0, 1], r_3 \in [0, 1]$
Gorilla troops optimizer (GTO)[41]	Control parameter $p = 0.03, \beta = 3, \omega = 0.8$
Prairie dog optimization algorithm (PDO)[89]	Account for individual PD difference $\rho = 0.005$; Food source alarm $epsPD = 0.1$
Sparrow search algorithm combining sine-cosine and cauchy mutation (SCSSA)[90]	Proportion of finders $PD = 0.3$; Proportion of investigators $SD = 0.1$; Alert threshold $R_2 = 0.8$
Crayfish optimization algorithm (COA)[42]	Decreasing coefficient $C_1 = 2$; Ambient temperature (15, 35);
	Coefficient of food size $C_2 = 3$; Coefficient of food intake $C_3 = 0.2$
Circulatory system based optimization (CSBO)[34]	Numbers of the weakest population; enter the pulmonary circulation $n/3$
Adaptive differential evolution with optional external archive (JADE)[16]	Mutation probability $ps = 0.5$; adjustment factor for the crossover process $c = 0.8$
Self-adaptive differential evolution with neighborhood search (SaNSDE)[15]	Initial value of crossover rate $CR = 0.5$; Factor of mutation $F = 0.5$; Neighborhood search factor $f_p = 0.5$

Table 6. CEAHA and 21 meta-heuristic optimization algorithms used for comparative analysis. *n* denotes the population size of the algorithm (the number of search agent individuals), *T* represents the maximum number of iterations, and *t* indicates the current moment during the iterative process

effectively execute meta-heuristic algorithms, intelligent agents must be broadly distributed across the entire search space during the exploration phase, while remaining focused during the exploitation phase. During the later stages of algorithm iteration, efforts should be made to minimize excessive clustering of intelligent agents to prevent the entire population from prematurely converging on local optima, an undesirable event. This paper employs the diversity measure formula proposed in the literature[86], which is as follows:

$$Div_z = \frac{1}{N} \sum_{i=1}^{N} |median(x^z) - x_i^z| \tag{17}$$

$$Div = \frac{1}{d} \sum_{z=1}^{d} Div_z \tag{18}$$

In Eqs. (17) and 18, *N* is population size, and *d* is the dimension of the solution space. x_i^z refers to the solution of the *i*-th hummingbird individual in the *z*-dimensional direction, while $median(x^z)$ denotes the median position of the entire population in the same *d*-dimensional space. Div_z represents the diversity of the population in specific *z*-dimension direction, and *Div* signifies the diversity index of the population across all dimensions. The larger the value of *Div*, the richer the diversity of the population. The rightmost columns of Figs. 5, 6 and 7 display the curves of average diversity over iterations for the eight different versions of CEAHA and the original AHA when addressing 23 test functions.

Fun	Index	CEAHA	AHA	DGSAHA	IAHA	LCAHA	AOA	COA	CS	CSBO	EEFO	EMA
CF1	Mean	1.27E+08	2.37E+08+	2.75E+08+	2.08E+08+	2.19E+08+	7.44E+09+	3.71E+08+	1.99E+10+	1.25E+08≈	2.52E+08+	1.79E+09+
	Std	3.79E+07	6.96E+07	6.57E+07	4.89E+07	5.19E+07	2.13E+09	1.16E+08	3.00E+09	3.18E+07	5.24E+07	7.97E+08
CF2	Mean	8.41E+07	4.28E+10+	1.02E+10+	2.66E+10+	2.79E+10+	3.03E+11+	5.05E+10+	6.02E+11+	1.23E+09+	1.02E+10+	8.35E+10+
	Std	2.42E+07	1.35E+10	4.99E+09	5.05E+09	9.11E+09	1.59E+10	1.12E+10	5.66E+10	7.42E+08	2.31E+09	1.44E+10
CF3	Mean	2.64E+04	8.06E+04+	9.00E+04+	5.48E+04+	4.91E+04+	2.96E+05+	5.76E+05+	8.61E+05+	3.72E+04+	8.87E+04+	7.52E+05+
	Std	2.74E+03	1.63E+04	1.24E+04	1.09E+04	7.17E+03	1.07E+04	1.03E+05	1.61E+05	8.48E+03	1.40E+04	8.68E+04
CF4	Mean	9.29E+02	4.48E+03+	2.19E+03+	2.99E+03+	3.08E+03+	9.59E+04+	6.74E+03+	2.62E+05+	1.01E+03+	2.38E+03+	1.19E+04+
	Std	5.61E+01	1.59E+03	1.02E+03	6.25E+02	5.68E+02	1.64E+04	3.23E+03	2.96E+04	7.31E+01	3.99E+02	3.59E+03
CF5	Mean	5.20E+02	5.21E+02+	5.21E+02+	5.21E+02+	5.20E+02+	5.21E+02+	5.21E+02+	5.21E+02+	5.21E+02+	5.21E+02+	5.21E+02+
	Std	3.66E-02	1.17E-01	3.29E-01	1.59E-01	1.65E-01	2.98E-02	8.11E-02	3.30E-02	2.88E-02	3.00E-02	2.41E-02
CF6	Mean	6.85E+02	7.05E+02+	7.03E+02+	6.98E+02+	6.99E+02+	7.55E+02+	7.32E+02+	7.72E+02+	7.43E+02+	7.14E+02+	7.39E+02+
	Std	5.59E+00	5.75E+00	3.92E+00	6.84E+00	6.48E+00	4.01E+00	9.17E+00	4.43E+00	4.18E+00	4.32E+00	1.49E+01
CF7	Mean	7.02E+02	1.10E+03+	7.80E+02+	9.69E+02+	9.63E+02+	3.72E+03+	1.18E+03+	6.16E+03+	7.13E+02+	8.05E+02+	1.49E+03+
	Std	2.50E-01	1.11E+02	5.51E+01	5.99E+01	7.67E+01	2.12E+02	1.36E+02	4.34E+02	5.49E+00	2.09E+01	1.46E+02
CF8	Mean	8.58E+02	1.31E+03+	1.17E+03+	1.26E+03+	1.25E+03+	2.29E+03+	1.53E+03+	2.74E+03+	1.51E+03+	1.35E+03+	1.58E+03+
	Std	2.42E+01	5.57E+01	1.94E+01	4.54E+01	4.09E+01	5.90E+01	4.82E+01	1.08E+02	2.78E+01	4.53E+01	5.65E+01
CF9	Mean	1.46E+03	1.74E+03+	1.63E+03+	1.64E+03+	1.64E+03+	2.34E+03+	1.78E+03+	3.29E+03+	1.87E+03+	1.65E+03+	2.25E+03+
	Std	4.29E+01	5.64E+01	4.20E+01	5.47E+01	3.77E+01	4.73E+01	3.91E+01	1.55E+02	3.26E+01	5.68E+01	8.45E+01
CF10	Mean	2.16E+03	1.10E+04+	6.58E+03+	7.71E+03+	8.33E+03+	2.99E+04+	1.87E+04+	3.48E+04+	2.31E+04+	1.40E+04+	1.77E+04+
	Std	6.07E+02	2.17E+03	7.58E+02	1.85E+03	1.93E+03	1.14E+03	2.22E+03	7.36E+02	4.80E+02	1.58E+03	1.58E+03
CF11	Mean	1.32E+04	1.57E+04+	1.48E+04+	1.54E+04+	1.56E+04+	3.06E+04+	2.29E+04+	3.50E+04+	3.08E+04+	1.90E+04+	3.35E+04+
	Std	1.21E+03	1.10E+03	8.23E+02	1.21E+03	1.05E+03	1.56E+03	2.66E+03	6.31E+02	5.55E+02	1.72E+03	6.25E+02
CF12	Mean	1.20E+03	1.20E+03+	1.20E+03+	1.20E+03+	1.20E+03+	1.20E+03+	1.20E+03+	1.21E+03+	1.20E+03+	1.20E+03+	1.20E+03+
	Std	4.79E-02	1.23E-01	3.44E-01	9.01E-02	1.22E-01	3.20E-01	4.88E-01	5.47E-01	3.03E-01	4.19E-01	3.05E-01
CF13	Mean	1.30E+03	1.30e+03+	1.30E+03+	1.30E+03+	1.30E+03+	1.31E+03+	1.30E+03+	1.31E+03+	1.30E+03+	1.30E+03+	1.30E+03+
	Std	6.44E-02	1.06E+00	8.52E-02	5.42E-01	3.80E-01	3.68E-01	1.09E+00	9.96E-01	4.31E-02	6.81E-02	4.03E-01
CF14	Mean	1.40E+03	1.49E+03+	1.42E+03+	1.46E+03+	1.46E+03+	2.06E+03+	1.47E+03+	2.72E+03+	1.40E+03+	1.43E+03+	1.59E+03+
	Std	2.22E-02	2.17E+01	2.32E+01	1.40E+01	1.21E+01	7.02E+01	2.38E+01	1.25E+02	3.54E-02	1.22E+01	3.74E+01
CF15	Mean	1.60E+03	4.14E+04+	7.37E+03+	1.49E+04+	1.26E+04+	2.13E+07+	5.77E+04+	5.15E+08+	1.68E+03+	8.71E+03+	1.31E+06+
	Std	2.02E+01	2.09E+04	7.28E+03	7.63E+03	5.68E+03	8.36E+06	3.83E+04	1.82E+08	3.58E+01	4.51E+03	8.70E+05
CF16	Mean	1.64E+03	1.64E+03+	1.64E+03+	1.64E+03+	1.64E+03+	1.65E+03+	1.65E+03+	1.65E+03+	1.65E+03+	1.65E+03+	1.65E+03+
	Std	1.09E+00	1.08E+00	5.11E-01	8.58E-01	1.14E+00	3.38E-01	4.75E-01	2.80E-01	2.87E-01	7.41E-01	2.52E-01
CF17	Mean	2.93E+07	5.59E+07+	5.17E+07+	4.27E+07+	4.14E+07+	1.07E+09+	4.38E+07+	2.88E+09+	6.15E+06-	3.59E+07≈	2.01E+08+
	Std	8.89E+06	1.82E+07	1.01E+07	1.69E+07	1.50E+07	3.76E+08	2.11E+07	7.68E+08	2.25E+06	1.77E+07	1.03E+08
CF18	Mean	1.10E+06	4.06E+07+	3.41E+07+	6.60E+06+	5.96E+06+	3.94E+10+	8.75E+07+	7.49E+10+	4.09E+03-	2.22E+06+	6.42E+07+
	Std	3.42E+06	4.47E+07	1.11E+08	3.88E+06	2.65E+06	7.09E+09	2.30E+08	9.90E+09	1.74E+03	1.17E+06	9.02E+07
CF19	Mean	2.06E+03	2.21E+03+	2.12E+03+	2.12E+03+	2.11E+03+	8.90E+03+	2.19E+03+	2.15E+04+	2.03E+03-	2.13E+03+	2.17E+03+
	Std	3.20E+01	6.65E+01	3.92E+01	4.43E+01	3.52E+01	1.50E+03	6.44E+01	3.76E+03	1.87E+01	3.27E+01	6.99E+01
CF20	Mean	7.04E+04	1.06E+05+	1.08E+05+	1.16E+05+	1.25E+05+	7.90E+05+	4.34E+05+	2.69E+07+	4.30E+04-	1.11E+05+	1.55E+06+
	Std	1.41E+04	1.66E+04	1.66E+04	2.04E+04	2.26E+04	3.31E+05	2.49E+05	1.77E+07	1.51E+04	2.23E+04	7.84E+05

Continued

Fun	Index	CEAHA	AHA	DGSAHA	IAHA	LCAHA	AOA	COA	CS	CSBO	EEFO	EMA
CF21	Mean	1.11E+07	1.86E+07+	2.05E+07+	1.22E+07+	1.27E+07≈	4.15E+08+	1.30E+07≈	1.36E+09+	2.61E+06-	1.09E+07≈	9.02E+07+
	Std	3.58E+06	8.14E+06	3.96E+06	4.56E+06	5.63E+06	1.89E+08	5.31E+06	3.71E+08	1.43E+06	4.66E+06	5.42E+07
CF22	Mean	4.81E+03	5.23E+03+	4.50E+03	5.03E+03≈	4.93E+03≈	1.32E+05+	5.42E+03+	1.56E+06+	6.45E+03+	4.69E+03≈	7.57E+03+
	Std	5.01E+02	5.99E+02	4.40E+02	5.47E+02	5.78E+02	1.09E+05	7.20E+02	1.05E+06	3.28E+02	5.17E+02	2.82E+02
CF23	Mean	2.50E+03	2.50E+03≈	2.50E+03≈	2.50E+03≈	2.50E+03≈	2.50E+03≈	2.50E+03≈	1.08E+04+	2.66E+03+	2.50E+03≈	2.92E+03+
	Std	0.00E+00	0.00E+00	0.00E+00	0.00E+00	0.00E+00	9.11E-01	0.00E+00	1.46E+03	4.08E+00	0.00E+00	8.37E+01
CF24	Mean	2.60E+03	2.60E+03≈	2.60E+03≈	2.60E+03≈	2.60E+03≈	2.60E+03+	2.60E+03≈	4.28E+03+	2.81E+03+	2.60E+03+	2.87E+03+
	Std	0.00E+00	0.00E+00	0.00E+00	0.00E+00	0.00E+00	2.13E-01	0.00E+00	1.70E+02	8.41E+00	1.75E-06	1.23E+02
CF25	Mean	2.70E+03	2.70E+03≈	2.70E+03≈	2.70E+03≈	2.70E+03≈	2.70E+03+	2.70E+03≈	4.14E+03+	2.78E+03+	2.70E+03≈	2.73E+03+
	Std	0.00E+00	0.00E+00	0.00E+00	0.00E+00	0.00E+00	2.89E-02	0.00E+00	1.38E+02	1.12E+01	0.00E+00	2.38E+01
CF26	Mean	2.80E+03	2.80E+03≈	2.80E+03≈	2.80E+03≈	2.80E+03≈	2.80E+03+	2.80E+03≈	4.06E+03+	2.80E+03+	2.80E+03≈	2.82E+03+
	Std	0.00E+00	0.00E+00	0.00E+00	0.00E+00	0.00E+00	2.73E-04	0.00E+00	2.05E+02	6.96E-01	0.00E+00	7.58E+01
CF27	Mean	2.90E+03	2.90E+03≈	2.90E+03≈	2.90E+03≈	2.90E+03≈	9.13E+03+	2.90E+03≈	8.85E+03+	4.83E+03+	2.90E+03≈	6.02E+03+
	Std	2.31E-12	2.31E-12	2.31E-12	2.31E-12	2.31E-12	7.51E+02	2.31E-12	5.52E+02	3.83E+02	2.31E-12	2.26E+02
CF28	Mean	3.00E+03	3.00E+03≈	3.00E+03≈	3.00E+03≈	3.00E+03≈	3.15E+04+	3.00E+03≈	3.87E+04+	7.73E+03+	3.00E+03≈	7.02E+03+
	Std	2.31E-12	2.31E-12	2.31E-12	2.31E-12	2.31E-12	1.46E+04	2.31E-12	2.83E+03	9.30E+02	2.31E-12	9.62E+02
CF29	Mean	3.10E+03	3.10E+03≈	3.10E+03≈	3.10E+03≈	3.10E+03≈	3.40E+09+	3.10E+03≈	5.88E+09+	7.41E+07+	3.10E+03≈	7.43E+07+
	Std	0.00E+00	0.00E+00	0.00E+00	0.00E+00	0.00E+00	2.51E+09	0.00E+00	1.02E+09	3.62E+07	0.00E+00	2.39E+07
CF30	Mean	3.20E+03	3.20E+03≈	3.20E+03≈	3.20E+03≈	3.20E+03≈	2.04E+08+	3.20E+03≈	3.72E+08+	5.47E+04+	3.22E+05+	4.59E+05+
	Std	0.00E+00	0.00E+00	0.00E+00	0.00E+00	0.00E+00	1.12E+08	0.00E+00	1.05E+08	2.53E+04	7.71E+05	2.17E+05
CEAHA wins	+		22	21	20	20	30	21	30	24	21	30
Similar	≈		8	8	10	10	0	9	0	1	9	0
Competitor wins	-		0	1	0	0	0	0	0	5	0	0

Fun	Index	GOA	GTO	PDO	PSO	SCSSA	SHCO	SPBO	SSA	WOA	JADE	SaNSDE
CF1	Mean	5.25E+08+	1.65E+08+	8.25E+09+	2.39E+10+	4.89E+08+	1.01E+09+	2.66E+08+	6.38E+07+	2.90E+08+	1.75E+09+	1.72E+08+
	Std	1.23E+08	3.85E+07	2.01E+09	4.07E+09	7.15E+07	2.49E+08	7.22E+07	2.65E+07	8.25E+07	5.61E+08	3.55E+07
CF2	Mean	6.09E+10+	8.42E+09+	2.77E+11+	6.42E+11+	6.99E+10+	1.12E+11+	3.33E+10+	2.77E+05-	1.72E+10+	1.11E+11+	3.11E+08+
	Std	1.42E+10	5.48E+09	1.43E+10	3.00E+10	1.22E+10	1.46E+10	5.58E+09	3.10E+05	4.62E+09	7.13E+10	1.00E+08
CF3	Mean	3.77E+05+	1.09E+05+	3.82E+05+	2.67E+06+	2.66E+05+	3.09E+05+	4.90E+04+	1.46E+05+	1.57E+05+	3.86E+05+	1.68E+05+
	Std	7.91E+04	2.08E+04	9.17E+04	7.02E+06	2.15E+04	2.99E+04	9.95E+03	3.79E+04	3.08E+04	6.41E+04	6.39E+04
CF4	Mean	4.97E+03+	1.64E+03+	9.43E+04+	3.08E+05+	7.80E+03+	1.54E+04+	6.68E+03+	6.69E+02+	2.76E+03+	2.76E+04+	9.36E+02≈
	Std	1.52E+03	3.95E+02	8.18E+03	2.95E+04	1.87E+03	5.30E+03	1.96E+03	1.12E+02	7.40E+02	1.26E+04	4.36E+01

Fun	Index	GOA	GTO	PDO	PSO	SCSSA	SHCO	SPBO	SSA	WOA	SaNSDE	JADE
CF5	Mean	5.21E+02+	5.21E+02+	5.21E+02+	5.21E+02+	5.21E+02+	5.21E+02+	5.21E+02+	5.20E+02≈	5.21E+02+	5.21E+02+	5.21E+02+
	Std	5.19E−02	2.97E−01	6.93E−02	3.79E−02	2.38E−01	2.40E−02	7.73E−02	1.06E−01	7.78E−02	9.99E−02	2.79E−02
CF6	Mean	7.20E+02+	7.36E+02+	7.59E+02+	7.77E+02+	7.23E+02+	7.30E+02+	6.68E+02+	6.49E+02+	6.70E+02+	7.34E+02+	7.26E+02+
	Std	8.62E+00	8.49E+00	4.38E+00	3.86E+00	6.72E+00	7.39E+00	3.10E+00	4.94E+00	4.56E+00	4.67E+00	2.79E+00
CF7	Mean	1.20E+03+	7.73E+02+	3.51E+03+	6.60E+03+	1.40E+03+	1.86E+03+	1.07E+03+	7.00E+02-	8.59E+02+	7.04E+02+	1.76E+03+
	Std	1.15E+02	4.46E+01	1.26E+02	3.91E+02	1.64E+02	1.70E+02	7.57E+01	1.84E−01	3.95E+01	1.08E+00	6.34E+02
CF8	Mean	1.73E+03+	1.39E+03+	2.16E+03+	2.83E+03+	1.58E+03+	1.84E+03+	1.33E+03+	1.11E+03+	1.26E+03+	1.39E+03+	1.77E+03+
	Std	5.07E+01	4.19E+01	8.66E+01	5.97E+01	7.05E+01	5.42E+01	4.09E+01	4.28E+01	6.55E+01	4.34E+01	1.24E+02
CF9	Mean	2.02E+03+	1.61E+03+	2.21E+03+	3.42E+03+	1.85E+03+	2.09E+03+	1.53E+03+	1.23E+03+	1.47E+03+	1.83E+03+	2.07E+03+
	Std	9.49E+01	5.27E+01	9.76E+01	1.21E+02	4.04E+01	9.41E+01	4.34E+01	7.66E+01	8.18E+01	4.47E+01	2.67E+02
CF10	Mean	2.16E+04+	1.47E+04+	3.09E+04+	3.57E+04+	1.81E+04+	2.60E+04+	1.28E+04+	8.06E+03+	1.12E+04+	1.98E+04+	2.30E+04+
	Std	1.50E+03	2.54E+03	1.14E+03	7.42E+02	2.07E+03	1.31E+03	9.58E+02	9.55E+02	9.06E+02	9.24E+02	6.83E+02
CF11	Mean	2.25E+04+	1.70E+04+	3.10E+04+	3.58E+04+	2.18E+04+	2.87E+04+	1.39E+04+	7.99E+03+	1.29E+04+	2.88E+04+	2.53E+04+
	Std	1.43E+03	2.03E+03	1.60E+03	9.55E+02	3.88E+03	1.42E+03	7.91E+02	8.90E+02	1.16E+03	1.50E+03	5.44E+02
CF12	Mean	1.20E+03+	1.20E+03+	1.20E+03+	1.21E+03+	1.20E+03+	1.20E+03+	1.20E+03+	1.20E+03+	1.20E+03+	1.20E+03+	1.20E+03+
	Std	7.05E−01	6.62E−01	6.06E−01	5.95E−01	1.14E+00	3.64E−01	5.82E−01	4.28E−01	6.07E−01	8.83E−01	1.56E−01
CF13	Mean	1.30E+03+	1.30E+03+	1.31E+03+	1.31E+03+	1.30E+03+	1.31E+03+	1.30E+03+	1.30E+03+	1.30E+03+	1.30E+03+	1.30E+03+
	Std	8.22E−01	7.50E−02	2.51E−01	6.19E−01	3.50E−01	3.67E−01	3.99E−01	1.59E−01	9.71E−01	6.63E−02	2.39E+00
CF14	Mean	1.49E+03+	1.42E+03+	2.04E+03+	2.81E+03+	1.51E+03+	1.61E+03+	1.49E+03+	1.40E+03+	1.43E+03+	1.40E+03+	1.69E+03+
	Std	2.09E+01	1.97E+01	4.90E+01	1.04E+02	2.13E+01	2.75E+01	1.92E+01	2.09E−01	1.10E+01	6.87E−02	1.39E+02
CF15	Mean	1.61E+05+	3.42E+03+	1.84E+07+	7.44E+08+	1.24E+05+	4.65E+05+	1.10E+05+	1.55E+03+	6.02E+04+	1.64E+03+	1.56E+07+
	Std	1.14E+05	2.00E+03	7.42E+06	2.08E+08	6.71E+04	2.69E+05	7.46E+04	1.34E+01	3.12E+04	2.66E+01	9.95E+06
CF16	Mean	1.65E+03+	1.64E+03+	1.65E+03+	1.65E+03+	1.65E+03+	1.65E+03+	1.62E+03+	1.62E+03+	1.62E+03+	1.65E+03+	1.64E+03+
	Std	7.58E−01	8.74E−01	7.72E−01	2.84E−01	6.82E−01	3.97E−01	3.24E−01	4.95E−01	4.76E−01	5.98E−01	4.21E−01
CF17	Mean	3.36E+07≈	1.03E+07-	1.43E+09+	4.05E+09+	6.15E+07+	1.27E+08+	1.01E+07+	4.81E+06+	1.43E+08+	1.27E+07-	3.78E+08+
	Std	1.44E+07	4.21E+06	3.87E+08	1.21E+09	2.59E+07	5.03E+07	4.97E+06	2.44E+06	6.76E+07	6.50E+06	1.21E+08
CF18	Mean	2.98E+06+	5.44E+05-	3.62E+10+	8.47E+10+	6.58E+07+	6.43E+09+	1.23E+08+	4.56E+03≈	5.28E+07+	3.78E+03-	1.35E+10+
	Std	2.53E+06	2.36E+06	5.94E+09	1.26E+10	6.71E+07	3.51E+09	7.64E+07	1.63E+03	9.53E+07	6.77E+02	7.80E+09
CF19	Mean	2.15E+03+	2.11E+03+	9.46E+03+	2.60E+04+	2.21E+03+	3.06E+03+	2.08E+03+	1.96E+03≈	2.20E+03+	2.02E+03-	3.77E+03+
	Std	8.16E+01	5.54E+01	1.60E+03	5.55E+03	9.14E+01	4.97E+02	4.01E+01	2.14E+01	8.60E+01	1.67E+01	6.55E+02
CF20	Mean	1.95E+05+	6.16E+04-	1.83E+06+	5.83E+07+	2.44E+05+	3.20E+05+	1.31E+04+	6.24E+04+	8.71E+05+	1.82E+05+	1.15E+06+
	Std	6.55E+04	1.71E+04	1.49E+06	3.57E+07	5.94E+04	1.31E+05	5.70E+03	2.56E+04	8.27E+05	1.08E+05	5.72E+05

Fun	Index	GOA	GTO	PDO	PSO	SCSSA	SHCO	SPBO	SSA	WOA	SaNSDE	JADE
CF21	Mean	1.73E+07+	4.32E+06-	4.40E+08+	2.21E+09+	1.49E+07+	5.50E+07+	2.41E+06+	3.19E+06+	2.69E+07+	6.28E+06-	2.69E+08+
	Std	1.05E+07	1.34E+06	1.41E+08	6.65E+08	6.13E+06	2.22E+07	9.13E+05	2.03E+06	1.79E+07	3.86E+06	1.31E+08
CF22	Mean	5.03E+03≈	5.28E+03+	1.09E+05+	2.23E+06+	5.16E+03≈	7.17E+03+	4.66E+03+	3.47E+03≈	5.01E+03+	6.61E+03+	4.67E+04+
	Std	5.68E+02	5.58E+02	8.30E+04	1.74E+06	7.73E+02	1.93E+03	4.46E+02	3.96E+02	1.03E+03	2.77E+02	5.07E+04
CF23	Mean	2.92E+03+	2.50E+03≈	2.50E+03≈	1.22E+04+	2.50E+03≈	2.50E+03≈	2.58E+03+	2.71E+03+	2.86E+03+	2.66E+03+	3.73E+03+
	Std	6.40E+01	0.00E+00	0.00E+00	1.46E+03	0.00E+00	0.00E+00	1.03E+02	1.81E+01	1.37E+02	3.53E+00	6.74E+02
CF24	Mean	2.99E+03+	2.60E+03+	2.60E+03≈	4.39E+03+	2.60E+03≈	2.60E+03≈	2.61E+03+	2.70E+03+	2.60E+03+	2.81E+03+	3.37E+03+
	Std	4.48E+01	2.69E-09	0.00E+00	1.84E+02	0.00E+00	0.00E+00	1.80E+01	8.88E+00	1.75E+00	5.47E+00	2.51E+02
CF25	Mean	2.82E+03+	2.70E+03≈	2.70E+03≈	4.35E+03+	2.70E+03≈	2.70E+03≈	2.70E+03+	2.74E+03+	2.70E+03+	2.79E+03+	2.91E+03+
	Std	2.26E+01	0.00E+00	0.00E+00	2.77E+02	0.00E+00	0.00E+00	7.74E-01	7.28E+00	1.05E+01	1.01E+01	6.55E+01
CF26	Mean	2.81E+03+	2.80E+03≈	2.80E+03≈	4.39E+03+	2.80E+03≈	2.80E+03≈	2.73E+03-	2.70E+03-	2.71E+03-	2.81E+03≈	2.79E+03≈
	Std	5.28E+00	1.81E+01	0.00E+00	2.35E+02	0.00E+00	0.00E+00	4.38E+01	1.94E+01	2.48E+01	1.90E+00	9.92E+01
CF27	Mean	6.09E+03+	2.90E+03≈	7.81E+03+	1.12E+04+	2.90E+03≈	2.90E+03≈	4.04E+03+	4.21E+03+	4.95E+03+	5.10E+03+	6.44E+03+
	Std	2.24E+02	2.31E-12	1.31E+02	1.85E+03	2.31E-12	2.31E-12	1.02E+03	1.23E+02	1.09E+02	2.61E+02	8.53E+01
CF28	Mean	1.05E+04+	3.00E+03≈	2.78E+04+	4.32E+04+	3.00E+03≈	3.00E+03≈	6.09E+03+	5.72E+03+	8.73E+03+	7.59E+03+	8.57E+03+
	Std	1.12E+03	2.31E-12	8.98E+03	2.84E+03	2.31E-12	2.31E-12	4.16E+03	8.76E+02	2.19E+03	1.62E+03	6.38E+02
CF29	Mean	8.44E+08+	3.10E+03≈	9.59E+08+	9.68E+09+	3.10E+03≈	3.10E+03≈	2.31E+08+	8.26E+07+	8.27E+07+	7.83E+04+	8.51E+07+
	Std	9.30E+08	0.00E+00	1.40E+08	1.23E+09	0.00E+00	0.00E+00	2.03E+08	9.70E+07	5.99E+07	3.67E+04	3.01E+06
CF30	Mean	1.88E+06+	2.32E+05+	1.98E+08+	5.89E+08+	3.20E+03≈	3.20E+03≈	2.08E+06+	1.08E+05+	1.23E+06+	1.38E+05+	7.80E+06+
	Std	8.78E+05	6.62E+05	7.93E+07	1.92E+08	0.00E+00	0.00E+00	2.62E+06	8.29E+04	1.07E+06	4.81E+04	2.96E+06
CEAHA wins		28	20	26	30	21	22	28	23	29	25	29
Similar		2	6	4	0	9	8	0	4	0	1	1
Competitor wins		0	4	0	0	0	0	2	3	1	4	0

Table 7. Statistical results of CEAHA compared with other optimization algorithms in CEC2014 (100D).

From the convergence curves of Figs. 5, 6 and 7, it is observed that the eight versions of CEAHA all outperform the original AHA across 23 standard benchmark functions. A detailed analysis of unimodal problems reveals that CEAHA must swiftly guide the population to resource-rich regions in the early stages, avoiding prolonged stagnation in flat or locally optimal areas. From F1 to F4 and F6, chaotic maps with U-shaped distributions exhibit rapid convergence due to their diversity curves quickly narrowing toward the optimal regions. For problems like F5 with large flat zones, the Circle map shows superior search performance.

For complex multimodal problems, featuring numerous local optima and high-dimensional challenges, maintaining a high level of diversity among the intelligent agents in the solution space is crucial. The results from F7, F9 to F12, and F16 to F18 indicate that the three chaotic maps with U-shaped distributions not only demonstrate better search performance but also maintain higher population diversity. For F13, however, the 2D-NHM chaotic system, characterized by its Spike distribution, shows a faster convergence rate and a slower convergence of population diversity. As for F17, with optima at the edge, the Logistic map succeeds in finding the best solution due to consistently highest population diversity. Since F19 and F20 are similar, as are F21, F22 and F23, with their search convergence and diversity curves nearly identical, only F19 and F23 are illustrated in Fig. 7. These problems are marked by significant differences between the minimum and other values, which is why, despite Chebyshev, Logistic, and Cubic maps maintaining high levels of population diversity, the 2D-NHM and Circle mappings exhibit better search convergence behavior.

Additionally, the Wilcoxon rank-sum test is utilized to evaluate the performance differences in solving 23 test functions among CEAHA-Cubic, the other seven versions of CEAHA, and the original AHA, as shown in Table 5. Initially, it is observed that the Cubic map, along with Logistic and Chebyshev maps, exhibits remarkably similar optimization performances. Subsequently, compared to other versions of CEAHA, the CEAHA version that incorporates the Cubic map demonstrates superior performance on all unimodal test problems and some multimodal test problems.

In summary, chaotic maps with U-shaped distributions, such as the Logistic, Chebyshev, and Cubic maps that engender chaotic traversal flight behavior, show outstanding performance in accelerating convergence while also maintaining population vitality and diversity. The traversal flight behavior with these chaotic maps significantly enhances the robustness and adaptability of the algorithms.

Performance of CEAHA with cubic map

The conclusion from previous section suggests that chaotic maps with a U-shaped distribution of the invariant probability measure f^* are more suitable for the design of chaotic traversal flights. Although the Cubic, Chebyshev, and Logistic exhibit similar curve shapes, there are slight differences in traversal efficiency when the population size is set to $N = 50$, with Cubic marginally outperforming Chebyshev, which in turn slightly surpasses Logistic (see Fig. 3). Therefore, Cubic map is selected to be the baseline pattern for the CEAHA chaotic traversal flight strategy. Concurrently, this version of CEAHA is comprehensively compared with three newly proposed AHA-based enhanced Hummingbird algorithms and other 17 meta-heuristic algorithms on the CEC2014, CEC2019, and the latest single-objective test suite CEC2022. Table 6 provides detailed listings of the names and parameter settings for 22 algorithms, with the parameter values for 21 competitive algorithms extracted from their respective original publications.

Wilcoxon rank sum test
To comprehensively assess the performance of the CEAHA, the Wilcoxon signed-rank test[91] is employed for comparative analysis. The significance level is set to $p = 0.05$. Here, "$\approx$" denotes no significant difference in the statistical sense, "+" to suggest that the corresponding CEAHA has surpassed the original AHA in performance, and "-" indicates the reverse situation. All considered algorithms are compared using the mean (Mean) and standard deviation (Std) of the best solutions obtained so far as two evaluation criteria. The formulas of Mean and Std are as follows:

$$Mean = \frac{1}{T}\sum_{i=1}^{T} P_i^*$$ (19)

$$Std = \sqrt{\frac{1}{T}(P_i^* - Mean)^2}$$ (20)

where P_i^* represents the best-so-far solution obtained in the i-th independent experimental run, and T denotes the number of independent experimental runs. The smaller the mean, the closer the feasible solution obtained by the algorithm is to the standard solution (true value), indicating that the algorithm possesses superior average performance. Moreover, the smaller the standard deviation, the more stable and reliable the feasible solution provided by the algorithm.

Table 7 showcases the assessment results on the 100-dimensional CEC2014 benchmark suite, with CEAHA outperforming AHA, DGSAHA, IAHA, LCAHA, COA, EEFO, and SHCO in nearly two-thirds of the test cases. Despite slightly lagging behind CSBO, SaNSDE, SSA, SPBO, and GTO in a few instances, CEAHA's performance is significantly superior to these algorithms on most test cases, especially when compared to AOA, CS, EMA, JADE, and GOA. Table 8 documents the performance of the algorithms on the CEC2019 test suite at specific dimensions, with CEAHA excelling in over half of the test cases compared to AHA, DGSAHA, IAHA, LCAHA. And CEAHA outstrips the other competitors on most of the CEC2019 problems.

Fun	Index	CEAHA	AHA	DGSAHA	IAHA	LCAHA	AOA	COA	CS	CSBO	EEFO	EMA
CF1	Mean	1.00E+00	1.00E+00≈	1.00E+00≈	1.00E+00≈	1.00E+00≈	2.94E+04+	1.00E+00≈	6.88E+08+	1.00E+00+	1.00E+00+	1.79E+05+
	Std	0.00E+00	0.00E+00	0.00E+00	0.00E+00	0.00E+00	9.74E+04	0.00E+00	3.09E+08	1.04E-03	5.44E-11	3.41E-05
CF2	Mean	4.19E+00	4.33E+00+	4.38E+00+	4.35E+00+	4.41E+00+	1.02E+04+	4.78E+00+	2.05E+04+	2.49E+01+	4.34E+00+	1.23E+03+
	Std	1.42E-01	2.30E-01	2.84E-01	2.60E-01	3.01E-01	3.25E+03	3.40E-01	5.03E+03	2.86E+01	2.29E-01	9.58E+02
CF3	Mean	1.33E+00	1.58E+00+	1.53E+00+	1.41E+00+	1.51E+00+	9.65E+00+	7.21E+00+	1.18E+01+	5.85E+00+	2.40E+00+	3.63E+00+
	Std	1.66E-01	4.50E-01	1.58E-01	4.93E-03	3.65E-01	1.10E+00	1.99E+00	3.33E-01	7.28E-01	6.85E-01	2.16E+00
CF4	Mean	1.01E+01	1.70E+01+	2.11E+01+	2.05E+01+	2.04E+01+	4.87E+01+	3.44E+01+	1.16E+02+	1.71E+01+	1.25E+01+	1.80E+01+
	Std	3.99E+00	9.64E+00	7.81E+00	8.08E+00	8.32E+00	1.38E+01	2.07E+01	1.69E+01	3.38E+00	5.27E+00	7.47E+00
CF5	Mean	1.06E+00	1.07E+00≈	1.18E+00+	1.11E+00+	1.10E+00+	6.52E+01+	1.22E+00+	1.31E+02+	1.15E+00+	1.10E+00+	1.09E+00+
	Std	3.18E-02	5.64E-02	5.16E-02	6.90E-02	6.50E-02	2.11E+01	1.40E-01	4.32E+01	4.91E-02	5.64E-02	4.90E-02
CF6	Mean	1.26E+00	1.37E+00≈	1.28E+00+	1.09E+00-	1.44E+00≈	1.04E+01+	3.75E+00+	1.31E+01+	1.79E+00+	1.53E+00+	2.87E+00+
	Std	4.71E-01	4.72E-01	1.78E-01	2.57E-01	6.43E-01	1.54E+00	1.62E+00	1.02E+00	6.57E-01	6.89E-01	1.46E+00
CF7	Mean	2.13E+02	6.26E+02+	4.61E+02+	5.46E+02+	6.27E+02+	1.29E+03+	1.12E+03+	2.15E+03+	8.80E+02+	4.65E+02+	5.85E+02+
	Std	1.49E+02	2.23E+02	1.20E+02	2.11E+02	1.81E+02	2.74E+02	3.78E+02	2.22E+02	1.46E+02	1.88E+02	2.42E+02
CF8	Mean	2.51E+00	3.30E+00+	3.42E+00+	3.55E+00+	3.34E+00+	4.69E+00+	3.90E+00+	5.24E+00+	4.00E+00+	3.52E+00+	3.68E+00+
	Std	4.80E-01	4.73E-01	2.96E-01	4.68E-01	4.71E-01	3.91E-01	3.65E-01	1.26E-01	2.65E-01	4.56E-01	4.42E-01
CF9	Mean	1.12E+00	1.11E+00≈	1.20E+00+	1.13E+00≈	1.13E+00≈	2.32E+00+	1.31E+00+	5.11E+00+	1.21E+00+	1.19E+00+	1.25E+00+
	Std	4.67E-02	5.46E-02	4.28E-02	4.78E-02	7.03E-02	8.02E-02	8.40E-02	6.54E-01	3.67E-02	6.14E-02	8.16E-02
CF10	Mean	1.17E+01	1.91E+01+	1.73E+01+	1.84E+01+	1.77E+01+	2.11E+01+	1.96E+01+	2.17E+01+	2.12E+01+	2.00E+01+	2.12E+01+
	Std	1.00E+01	5.75E+00	7.52E+00	6.78E+00	7.58E+00	3.85E-02	4.66E+00	1.18E-01	5.31E-02	5.15E+00	1.00E-01
CEAHA wins	+		6	9	7	7	10	9	10	10	10	10
Similar	≈		4	1	2	3	0	1	0	0	0	0
Competitor wins	−		0	0	1	0	0	0	0	5	0	0

Fun	Index	GOA	GTO	PDO	PSO	SCSSA	SHCO	SPBO	SSA	WOA	SaNSDE	JADE
CF1	Mean	2.05E+06+	1.00E+00≈	1.00E+00≈	1.49E+09+	1.00E+00≈	1.00E+00≈	8.49E+01≈	1.58E+06+	1.10E+07+	2.10E+03+	1.40E+07+
	Std	2.45E+06	0.00E+00	0.00E+00	7.67E+08	0.00E+00	0.00E+00	4.60E+02	1.53E+06	1.23E+07	1.15E+04	7.52E+06
CF2	Mean	9.98E+02+	4.41E+00+	5.00E+00+	3.00E+04+	5.00E+00+	5.00E+00+	6.94E+01+	8.46E+02+	7.51E+03+	5.58E+02+	4.43E+03+
	Std	5.70E+02	2.74E-01	2.12E-06	8.57E+03	0.00E+00	6.23E-05	1.94E+02	7.06E+02	2.97E+03	5.87E+02	1.41E+03
CF3	Mean	8.44E+00+	1.38E+00+	7.47E+00+	8.99E+00+	3.16E+00+	6.85E+00+	5.32E+00+	3.39E+00+	5.60E+00+	4.99E+00+	5.95E+00+
	Std	2.16E+00	1.04E-01	1.83E+00	8.15E-01	2.05E+00	2.46E+00	1.43E+00	1.92E+00	2.10E+00	9.56E-01	9.67E-01
CF4	Mean	2.17E+01+	2.56E+01+	7.47E+01+	1.39E+02+	4.49E+01+	3.90E+01+	3.82E+01+	2.52E+01+	4.89E+01+	1.15E+01+	1.23E+01+
	Std	1.02E+01	9.69E+00	1.39E+01	1.94E+01	2.34E+01	1.49E+01	9.44E+00	1.09E+01	1.89E+01	1.88E+00	2.66E+00
CF5	Mean	1.27E+00+	1.28E+00+	5.52E+01+	1.90E+02+	1.19E+00+	7.05E+00+	2.49E+00+	1.24E+00+	2.07E+00+	1.13E+00+	1.40E+00+
	Std	1.68E-01	2.09E-01	2.07E+01	5.40E+01	1.13E-01	1.16E+01	4.24E-01	1.50E-01	3.91E-01	3.24E-02	2.24E-01
CF6	Mean	4.63E+00+	4.74E+00+	1.06E+01+	1.51E+01+	4.08E+00+	6.18E+00+	7.04E+00+	4.23E+00+	8.59E+00+	1.18E+00≈	5.12E+00+
	Std	1.98E+00	1.30E+00	1.17E+00	9.62E-01	1.65E+00	1.53E+00	1.18E+00	2.34E+00	1.68E+00	1.98E-01	6.64E-01
CF7	Mean	1.00E+03+	9.12E+02+	1.70E+03+	2.48E+03+	1.25E+03+	1.03E+03+	1.20E+03+	1.04E+03+	1.25E+03+	4.71E+02+	8.34E+02+
	Std	2.21E+02	2.73E+02	3.08E+02	2.43E+02	3.61E+02	3.32E+02	2.17E+02	3.11E+02	3.07E+02	1.37E+02	2.54E+02
CF8	Mean	4.11E+00+	3.97E+00+	4.87E+00+	5.24E+00+	4.10E+00+	4.42E+00+	4.32E+00+	4.18E+00+	4.63E+00+	3.63E+00+	4.29E+00+
	Std	4.37E-01	4.71E-01	2.23E-01	1.94E-01	3.95E-01	3.73E-01	2.80E-01	3.03E-01	3.61E-01	1.87E-01	3.67E-01

Continued

Fun	Index	GOA	GTO	PDO	PSO	SCSSA	SHCO	SPBO	SSA	WOA	SaNSDE	JADE
CF9	Mean	1.28E+00+	1.21E+00+	3.00E+00+	5.76E+00+	1.32E+00+	1.40E+00+	1.40E+00+	1.37E+00+	1.34E+00+	1.20E+00+	1.26E+00+
	Std	1.13E−01	7.48E−02	8.70E−01	7.28E−01	1.33E−01	1.34E−01	1.49E−01	1.68E−01	1.65E−01	3.78E−02	5.02E−02
CF10	Mean	2.11E+01+	2.11E+01+	2.13E+01+	2.18E+01+	2.07E+01+	2.15E+01+	2.12E+01+	2.03E+01+	2.13E+01+	2.11E+01+	2.11E+01+
	Std	7.50E−02	1.24E−01	1.49E−01	1.34E−01	3.29E+00	1.03E−01	8.70E−02	3.65E+00	1.36E−01	2.64E−01	2.67E−02
CEAHA wins		10	9	9	10	9	9	9	10	10	9	10
Similar		0	1	1	0	1	1	1	0	0	1	0
Competitor wins		0	0	0	0	0	0	0	0	0	0	0

Table 8. Statistical results of CEAHA compared with other optimization algorithms in CEC2019.

On the 10-dimensional CEC2022 benchmark suite, as indicated in Table 9, CEAHA falls short of JADE in 7 out of 12 cases but leads AHA, DGSAHA, IAHA, LCAHA, EEFO, EMA, GOA, GTO, SPBO, SSA, and JADE in nearly two-thirds of the cases and outperforms AOA, WOA, and SHCO in the majority. Tables 10 and 11 reveal that on the 20-dimensional CEC2022 test suite, CEAHA's performance improves compared to the 10-dimensional case, slightly outdoing JADE in 8/12 cases, COA in 6/12 cases, and surpassing DGSAHA and GOA in nearly 9/12 of the cases, outperforming all other competitor algorithms in most cases. It is evident that CEAHA generally exhibits superior optimization capability when facing high-dimensional test problems.

Convergence and robustness analysis
To assess the convergence speed and robustness of various algorithms during the evolutionary process, Figs. 8 and 9 display the best fitness curves from 30 independent runs of CEAHA and 21 other competitive algorithms on the CEC2019 and CEC2022 test suites, all conducted with the same number of fitness evaluations (FES). Additionally, these figures also present box plots at the final fitness evaluation to demonstrate their performance outcomes. Additionally, to ensure fairness in comparison, all algorithms start from the same initial points, with a population size set at 50, and undergo 25,000 FES.

For the unimodal functions F1, F2, F5, and F9 within the CEC2019 suite, algorithms including CEAHA, DGSAHA, IAHA, LAHA, COA, GTO, EEFO and SCSSA exhibits rapid convergence. Notably, CEAHA demonstrates the highest optimization stability with the lowest median and narrowest interquartile range in its box plots. For F2, although SCSSA exhibited a superior best convergence curve earlier compared to CEAHA, and also performed exceptionally well in terms of robustness, this is merely an isolated extreme case. This is because, across other test functions, CEAHA generally shows better convergence performance and robustness than SCSSA. In the multimodal functions F3, F4, and F6 to F8, and F10 of CEC2019 test suite, CEAHA significantly shows the fastest convergence rate, consistently finding the optimal solutions, and also maintains superior stability in its box plots compared to other competitors. Specially, CEC2019-F7 is the Modified Schwefel's Function, characterized by its asymmetric search space which leads to unbalanced optimization paths and a global optimum not located at the center. In this problem, CEAHA quickly finds the optimal solution, followed by EEFO, EMA, and IAHA. CEAHA outperforms other algorithms on CEC2019-F7, demonstrating its ability to effectively handle asymmetry. CEC2019-F8 is the Expanded Schaffer's F6 Function, notable for the drastic and periodic changes in terrain near the global optimum area, which may cause cyclic search paths. CEAHA rapidly pinpoints the optimal solution in this case, while AHA gradually finds the solution after CEAHA's convergence. CEC2019-F10 is the Ackley Function, with a relatively flat central area challenging the algorithm's capability to explore regions with minor gradients. CEAHA, AHA, LCAHA, and EEFO manage to find the optimal solution within a limited number of function evaluations, and CEAHA has the best convergence rate compared with other competitive algorithms.

CEC2022 encompasses unimodal functions (F1), multimodal functions (from F2 to F5), composite functions (from F6 to F8), and constrained optimization functions (from F9 to F12). While CEAHA's convergence speed for F2 trails slightly behind IAHA, and its box plot shows a marginally higher stability compared to IAHA, DGSAHA, LCAHA, and SaNSDE, which indicates that CEAHA is still competitive. In the test functions F1, F3, F4, F5, F7, F9, and F12, CEAHA, IAHA, DGSAHA, and LCAHA demonstrated faster convergence speeds and more stable optimization performance compared to other competing algorithms such as JADE, SaNSDE, WOA, SSA, PSO, PDO, GTO, GOA, EMA, and AOA. A detailed analysis of Fig. 10 reveals that CEAHA's fitness evaluation curve converges the fastest, and its box plot at the 25,000th function evaluation shows the narrowest interquartile range, highlighting CEAHA's significant advantages in enhancing the convergence rate and robustness of performance in the artificial hummingbird algorithm. From these 12 test cases, it is evident that regardless of whether the problems are unimodal, multimodal, composite, or constrained optimization issues, CEAHA consistently maintains superior convergence speed and robustness.

Friedman test
To comprehensively and visually evaluate CEAHA against 21 other meta-heuristic competitor algorithms on CEC2014, CEC2019, and CEC2022 test suites, the Friedman test[92] is conducted. Figure 10 presents a bar chart of Friedman's mean ranks for CEAHA and its competitors across four dimensions (10D, 30D, 50D, and 100D) of the CEC2014 suite. CEAHA consistently ranks at the forefront across all tested dimensions with average ranks of 2.75, 3.5, 3.5, and 2.9, respectively, followed by IAHA, LCAHA, DGSAHA, EEFO, SaNSDE, GTO, CSBO, among others. Notably, as the dimension of problems increases, the average ranks of AOA, CSBO, EEFO, EMA, SPBO, SaNSDE, and JADE trend upward, while CEAHA maintains a strong performance with an average rank of only 2.9 in the challenging 100D tests, demonstrating its robust performance in high-dimensional optimization spaces.

Figure 11 depicts the Friedman's mean rank bar charts for CEAHA and competing algorithms on CEC2019 and the two dimensions (10D, 20D) of CEC2022. The data in the chart indicates that CEAHA leads the ranking, with an average rank of only 1.75 in CEC2019 and with average ranks of 3.33 and 3.67 in the 10D and 20D dimensions of CEC2022, respectively. These comparative results highlight that CEAHA shows exceptional potential and applicability in tackling non-convex problems in CEC2022, whether they are unimodal, multimodal, composite, or constrained optimization tasks.

Engineering cases analysis
To further validate the effectiveness of CEAHA in handling constrained global optimization problems, this section selects four practical engineering design challenges from existing literature. These problems include the design of pressure vessels, gear train, speed reducer, and piston lever. These design problems have been solved using various other optimization techniques. By comparing the results obtained with CEAHA to those

Fun	Index	CEAHA	AHA	DGSAHA	IAHA	LCAHA	AOA	COA	CS	CSBO	EEFO	EMA
CF1	Mean	3.00E+02	3.10E+02+	1.76E+03+	3.52E+02+	3.29E+02+	1.16E+04+	1.84E+03+	2.44E+04+	3.00E+02-	3.21E+02+	1.65E+03+
	Std	3.88E-02	2.25E+01	5.62E+02	1.10E+02	4.88E+01	4.59E+03	1.08E+03	6.34E+03	2.66E-08	3.17E+01	1.08E+03
CF2	Mean	4.04E+02	4.01E+02≈	4.00E+02≈	4.02E+02≈	4.02E+02≈	1.19E+03+	4.10E+02+	1.82E+03+	4.06E+02+	4.04E+02-	4.09E+02+
	Std	1.30E+01	2.85E+00	5.70E-02	2.88E+00	3.07E+00	4.99E+02	1.67E+01	6.98E+02	2.45E+00	3.84E+00	4.73E+00
CF3	Mean	6.02E+02	6.00E+02≈	6.00E+02≈	6.00E+02-	6.00E+02-	6.37E+02+	6.06E+02+	6.71E+02+	6.00E+02≈	6.00E+02≈	6.00E+02-
	Std	3.79E+00	2.93E-01	1.43E-02	2.85E-03	4.10E-03	7.61E+00	9.58E+00	1.09E+01	1.25E-03	1.53E-02	1.80E-01
CF4	Mean	8.24E+02	8.25E+02≈	8.27E+02+	8.27E+02+	8.26E+02≈	8.31E+02+	8.31E+02+	8.94E+02+	8.22E+02-	8.13E+02-	8.20E+02≈
	Std	5.62E+00	7.50E+00	6.43E+00	5.38E+00	6.01E+00	8.17E+00	5.47E+00	1.48E+01	3.55E+00	4.98E+00	1.21E+01
CF5	Mean	1.18E+03	9.21E+02-	1.06E+03-	9.16E+02-	9.01E+02-	1.39E+03+	1.01E+03-	3.14E+03+	9.00E+02-	9.01E+02-	9.01E+02-
	Std	1.72E+02	6.59E+01	2.20E+02	6.12E+01	1.68E+02	1.87E+02	1.96E+02	6.43E+02	6.18E-07	9.21E-01	1.98E+00
CF6	Mean	1.90E+03	1.91E+03≈	2.71E+03+	2.38E+03+	2.91E+03+	8.58E+03+	4.13E+03+	3.04E+08+	1.80E+03-	2.11E+03+	4.66E+03+
	Std	1.85E+02	2.63E+02	7.47E+02	8.71E+02	1.05E+03	2.41E+04	2.00E+03	2.22E+08	2.48E-01	6.43E+02	2.16E+03
CF7	Mean	2.01E+03	2.01E+03≈	2.01E+03≈	2.01E+03≈	2.01E+03≈	2.11E+03+	2.02E+03+	2.14E+03+	2.02E+03+	2.01E+03+	2.03E+03+
	Std	9.25E+00	9.97E+00	5.67E+00	9.52E+00	9.51E+00	4.09E+01	7.95E+00	2.62E+01	3.55E+00	9.43E+00	1.19E+01
CF8	Mean	2.21E+03	2.22E+03+	2.21E+03≈	2.22E+03+	2.22E+03+	2.26E+03+	2.22E+03+	2.32E+03+	2.22E+03+	2.22E+03+	2.22E+03+
	Std	8.64E+00	6.75E+00	6.89E+00	5.39E+00	3.98E+00	6.39E+01	6.78E+00	7.91E+01	4.09E+00	9.18E+00	4.94E+00
CF9	Mean	2.53E+03	2.53E+03+	2.51E+03-	2.53E+03+	2.53E+03+	2.73E+03+	2.53E+03+	2.83E+03+	2.53E+03-	2.53E+03+	2.53E+03-
	Std	2.45E-06	1.26E-02	1.05E+01	4.04E-03	2.39E-04	5.59E+01	2.05E-04	6.82E+01	2.23E-13	1.55E-03	6.40E-12
CF10	Mean	2.53E+03	2.52E+03-	2.56E+03+	2.52E+03-	2.53E+03+	2.65E+03+	2.54E+03+	2.95E+03+	2.52E+03-	2.50E+03≈	2.55E+03+
	Std	4.75E+01	3.79E+01	5.43E+01	4.27E+01	4.77E+01	1.79E+02	6.03E+01	2.82E+02	4.45E+01	2.10E+01	5.71E+01
CF11	Mean	2.60E+03	2.61E+03+	2.60E+03+	2.60E+03+	2.61E+03+	3.39E+03+	2.72E+03+	3.84E+03+	2.61E+03+	2.62E+03+	2.66E+03≈
	Std	5.26E-05	7.30E+01	2.10E-01	5.32E-03	5.48E+01	4.01E+02	1.34E+02	5.08E+02	7.30E+01	5.19E+01	7.32E+01
CF12	Mean	2.87E+03	2.87E+03≈	2.85E+03-	2.87E+03≈	2.87E+03≈	3.02E+03+	2.87E+03≈	2.99E+03+	2.86E+03-	2.87E+03≈	2.86E+03-
	Std	6.61E+00	2.40E+00	2.28E+00	2.65E+00	4.08E+00	6.20E+01	1.79E+00	6.41E+01	1.18E+00	2.08E+00	1.99E+00
CEAHA wins		+	4	5	6	6	12	10	12	4	6	6
Similar		≈	6	4	3	4	0	1	0	1	3	2
Competitor wins		–	2	3	3	2	0	1	0	7	3	4

Fun	Index	GOA	GTO	PDO	PSO	SCSSA	SHCO	SPBO	SSA	WOA	SaNSDE	JADE
CF1	Mean	3.00E+02+	3.00E+02-	1.20E+04+	2.78E+05+	5.74E+02+	3.59E+03+	5.51E+02+	3.00E+02-	2.50E+04+	4.49E+02≈	2.35E+04+
	Std	3.96E-01	1.09E-07	4.93E+03	7.83E+05	2.61E+02	2.91E+03	2.55E+02	7.75E-10	1.17E+04	3.91E+02	1.10E+04
CF2	Mean	4.06E+02+	4.09E+02+	9.92E+02+	3.02E+03+	4.11E+02+	4.52E+02+	4.32E+02+	4.07E+02+	4.56E+02+	4.05E+02+	4.10E+02+
	Std	3.33E+00	1.69E+01	3.47E+02	1.17E+03	1.75E+01	5.06E+01	3.11E+01	7.80E+00	7.41E+01	3.09E+00	1.17E+00
CF3	Mean	6.04E+02+	6.03E+02+	6.50E+02+	6.81E+02+	6.06E+02+	6.17E+02+	6.21E+02+	6.12E+02+	6.35E+02+	6.00E+02-	6.01E+02≈
	Std	5.22E+00	2.98E+00	8.72E+00	1.34E+01	1.17E+01	1.06E+01	7.06E+00	9.41E+00	1.18E+01	4.43E-05	3.08E-01
CF4	Mean	8.21E+02≈	8.20E+02-	8.48E+02+	9.10E+02+	8.30E+02+	8.38E+02+	8.28E+02+	8.21E+02≈	8.40E+02+	8.17E+02-	8.24E+02≈
	Std	9.17E+00	7.44E+00	9.46E+00	1.40E+01	7.46E+00	1.51E+01	8.81E+00	8.37E+00	1.48E+01	3.99E+00	6.88E+00
CF5	Mean	9.02E+02-	9.34E+02-	1.48E+03+	3.15E+03+	1.35E+03+	1.32E+03+	1.07E+03-	9.64E+02-	1.44E+03+	9.00E+02-	1.03E+03-
	Std	3.29E+00	2.99E+01	1.82E+02	6.60E+02	2.30E+02	2.31E+02	1.13E+02	1.47E+02	3.30E+02	1.15E-06	1.44E+02
CF6	Mean	3.76E+03+	1.90E+03+	8.61E+07+	1.14E+09+	3.28E+03+	1.73E+04+	3.54E+03+	4.27E+03+	5.13E+03+	1.80E+03-	1.94E+04+
	Std	1.82E+03	9.86E+01	1.84E+08	7.73E+08	1.56E+03	1.25E+04	1.92E+03	2.15E+03	2.57E+03	2.92E+00	1.12E+04

Continued

Fun	Index	GOA	GTO	PDO	PSO	SCSSA	SHCO	SPBO	SSA	WOA	SaNSDE	JADE
CF7	Mean	2.06E+03+	2.03E+03+	2.11E+03+	2.18E+03+	2.04E+03+	2.06E+03+	2.05E+03+	2.05E+03+	2.07E+03+	2.01E+03≈	2.02E+03+
	Std	3.85E+01	9.32E+00	3.84E+01	3.52E+01	3.22E+01	4.32E+01	1.07E+01	2.21E+01	2.89E+01	1.05E+00	3.54E+00
CF8	Mean	2.26E+03+	2.22E+03+	2.25E+03+	2.46E+03+	2.22E+03+	2.25E+03+	2.23E+03+	2.23E+03+	2.24E+03+	2.22E+03≈	2.22E+03+
	Std	5.66E+01	4.26E+00	2.47E+01	1.56E+02	9.13E+00	4.56E+01	2.62E+00	3.03E+00	1.24E+01	4.78E+00	2.41E+00
CF9	Mean	2.55E+03+	2.53E+03+	2.74E+03+	3.03E+03+	2.53E+03+	2.60E+03+	2.54E+03+	2.55E+03+	2.59E+03+	2.53E+03-	2.53E+03+
	Std	4.78E+01	2.68E+01	6.68E+01	2.09E+02	2.68E+01	4.24E+01	1.11E+01	3.67E+01	4.94E+01	1.70E-10	5.29E+00
CF10	Mean	2.62E+03+	2.51E+03-	2.59E+03+	3.60E+03+	2.56E+03+	2.62E+03+	2.50E+03-	2.51E+03-	2.60E+03+	2.50E+03≈	2.44E+03-
	Std	2.01E+02	3.86E+01	8.12E+01	7.18E+02	6.28E+01	1.33E+02	3.96E-01	3.80E+01	1.90E+02	5.50E-02	3.19E+01
CF11	Mean	2.73E+03+	2.65E+03+	3.22E+03+	4.74E+03+	2.74E+03+	2.89E+03+	2.71E+03+	2.65E+03+	2.82E+03+	2.60E+03-	2.73E+03+
	Std	1.73E+02	1.10E+02	3.42E+02	6.35E+02	2.18E+02	1.94E+02	4.24E+01	1.13E+02	1.51E+02	4.28E-06	4.79E+01
CF12	Mean	2.86E+03-	2.87E+03+	2.89E+03+	3.22E+03+	2.86E+03-	2.89E+03+	2.88E+03+	2.86E+03-	2.89E+03+	2.86E+03-	2.86E+03-
	Std	1.93E+00	1.56E+01	1.14E+01	1.26E+02	4.38E+00	2.45E+01	1.46E+01	1.68E+00	3.62E+01	9.69E-01	2.62E+00
CEAHA wins		9	8	12	12	11	12	10	7	12	1	7
Similar		1	0	0	0	0	0	0	1	0	4	2
Competitor wins		2	4	0	0	1	0	2	4	0	7	3

Table 9. Statistical results of CEAHA compared with other optimization algorithms in CEC2022(10D).

Fun	index	AHACLL	AHA	DGSAHA	IAHA	LCAHA	AOA	COA	CS	CSBO	EEFO	EMA	SaNSDE
CF1	Mean	7.86E+02	6.16E+03+	2.08E+04+	1.23E+04+	1.28E+04+	3.13E+04+	1.90E+03+	8.75E+04+	4.40E+02-	7.54E+03+	5.01E+04+	1.55E+04+
	Std	1.21E+02	2.43E+03	4.12E+03	6.33E+03	4.59E+03	8.69E+03	1.19E+03	4.53E+04	1.83E+02	2.69E+03	1.14E+04	1.20E+04
CF2	Mean	4.42E+02	4.67E+02+	4.43E+02≈	4.52E+02+	4.58E+02+	2.34E+03+	4.11E+02-	6.59E+03+	4.47E+02+	4.68E+02+	4.59E+02+	4.48E+02+
	Std	1.37E+01	4.75E+02	1.28E+02	4.85E+02	4.38E+02	4.11E+02	1.51E+02	1.32E+03	8.07E+00	2.19E+01	1.37E+01	1.80E+00
CF3	Mean	6.00E+02	6.01E+02+	6.00E+02+	6.01E+02+	6.01E+02+	6.64E+02+	6.03E+02+	7.06E+02+	6.00E+02+	6.02E+02+	6.01E+02+	6.00E+02+
	Std	2.05E-03	2.42E+00	3.59E-01	2.99E+00	2.35E+00	1.17E+01	5.42E+00	9.34E+00	3.16E-02	1.22E+00	1.39E+00	1.45E-02
CF4	Mean	8.42E+02	8.73E+02+	8.84E+02+	8.77E+02+	8.76E+02+	9.53E+02+	8.28E+02-	1.07E+03+	8.83E+02+	8.52E+02+	9.30E+02+	8.85E+02+
	Std	6.44E+00	1.81E+01	6.87E+00	1.52E+01	1.69E+01	1.74E+01	5.70E+00	2.91E+01	1.26E+01	1.76E+01	1.83E+01	1.64E+01
CF5	Mean	9.12E+02	1.89E+03+	2.43E+03+	1.81E+03+	1.87E+03+	2.98E+03+	9.82E+02≈	9.99E+03+	9.00E+02-	1.00E+03+	9.27E+02≈	9.00E+02-
	Std	4.97E+00	4.75E+02	1.28E+02	4.85E+02	4.38E+02	4.11E+02	1.51E+02	1.96E+03	3.05E-02	1.23E+02	3.30E+01	1.07E-01
CF6	Mean	1.96E+03	3.59E+03+	1.82E+04+	3.94E+03+	3.86E+03+	8.32E+08+	4.56E+03+	4.28E+09+	2.01E+03≈	4.75E+03+	6.10E+03+	1.40E+04+
	Std	1.11E+02	1.99E+03	1.45E+04	1.86E+03	2.47E+03	7.64E+08	1.78E+03	1.60E+09	6.28E+02	3.23E+03	5.03E+03	4.30E+04
CF7	Mean	2.02E+03	2.07E+03+	2.05E+03+	2.05E+03+	2.05E+03+	2.20E+03+	2.02E+03≈	2.36E+03+	2.06E+03+	2.05E+03+	2.07E+03+	2.05E+03+
	Std	4.32E+00	3.80E+01	1.22E+01	2.58E+01	1.45E+01	4.20E+01	5.14E+00	9.22E+01	9.08E+00	1.45E+01	3.12E+01	5.91E+00
CF8	Mean	2.22E+03	2.22E+03+	2.22E+03+	2.22E+03+	2.22E+03+	2.50E+03+	2.22E+03+	3.30E+03+	2.23E+03+	2.22E+03+	2.23E+03+	2.23E+03+
	Std	1.50E-01	4.97E+00	7.39E-01	3.05E+00	4.27E+00	2.26E+02	8.10E+00	1.03E+03	1.71E+00	2.22E+00	1.03E+01	2.66E+00
CF9	Mean	2.48E+03	2.49E+03+	2.47E+03-	2.48E+03+	2.48E+03+	3.22E+03+	2.53E+03+	3.51E+03+	2.48E+03-	2.48E+03+	2.48E+03≈	2.48E+03-
	Std	9.77E-02	3.80E+00	2.69E+00	1.88E+00	1.99E+00	2.66E+02	2.68E+02	3.18E+02	4.83E-06	2.25E+00	7.10E+00	7.70E-04
CF10	Mean	2.50E+03	2.53E+03+	2.51E+03+	2.53E+03+	2.54E+03+	5.41E+03+	2.55E+03+	6.51E+03+	2.62E+03+	2.53E+03+	2.98E+03+	2.52E+03+
	Std	5.76E-02	6.70E+01	2.54E+01	6.33E+01	8.39E+01	1.15E+03	5.98E+01	1.51E+03	3.36E+02	5.54E+01	5.07E+02	6.89E+01
CF11	Mean	2.85E+03	2.93E+03+	2.93E+03+	2.92E+03+	2.93E+03+	8.26E+03+	2.74E+03-	1.21E+04+	2.93E+03≈	2.95E+03+	2.96E+03+	2.93E+03≈
	Std	1.14E+02	1.11E+02	5.90E+01	7.16E+01	4.25E+01	9.18E+02	1.39E+02	1.68E+03	4.66E+01	5.84E+01	1.26E+02	5.00E+01
CF12	Mean	2.94E+03	2.98E+03+	2.91E+03-	2.97E+03+	2.96E+03+	3.79E+03+	2.87E+03-	3.76E+03+	2.94E+03-	2.97E+03+	2.95E+03+	2.94E+03≈
	Std	3.73E+00	1.62E+01	6.62E+00	1.54E+01	1.33E+01	2.11E+02	8.35E+00	2.12E+02	3.33E+00	1.90E+01	1.07E+01	6.72E+00
Chaos wins		+	12	9	12	12	12	6	12	6	12	10	8
Similar		≈	0	1	0	0	0	2	0	2	0	2	2
Competitor wins		−	0	2	0	0	0	4	0	4	0	0	2

Table 10. Statistical results of CEAHA compared with other optimization algorithms in CEC2022(20D).

Fun	index	AHACLL	AHA	GOA	GTO	PDO	PSO	SCSSA	SHCO	SPBO	SSA	WOA	JADE
CF1	Mean	7.86E+02	6.16E+03+	1.16E+03≈	4.40E+02-	7.39E+04+	1.13E+09+	5.07E+04+	1.81E+04+	1.36E+03+	3.92E+03+	3.02E+04+	6.66E+04+
	Std	1.21E+02	2.43E+03	1.16E+03	3.23E+02	2.12E+04	3.42E+09	2.31E+04	6.42E+03	4.93E+02	2.32E+03	9.79E+03	1.44E+04
CF2	Mean	4.42E+02	4.67E+02+	4.57E+02+	4.55E+02+	2.11E+03+	8.50E+03+	4.71E+02+	5.94E+02+	5.41E+02+	4.58E+02+	5.73E+02+	4.89E+02+
	Std	1.37E+01	1.51E+01	2.91E+01	2.02E+01	7.11E+02	2.15E+03	3.18E+01	1.05E+02	4.69E+01	1.61E+01	6.34E+01	1.68E+01
CF3	Mean	6.00E+02	6.01E+02+	6.28E+02+	6.29E+02+	6.78E+02+	7.16E+02+	6.34E+02+	6.43E+02+	6.51E+02+	6.37E+02+	6.68E+02+	6.09E+02+
	Std	2.05E-03	2.42E+00	1.18E+01	1.12E+01	9.38E+00	1.34E+01	1.89E+01	1.30E+01	9.55E+00	1.29E+01	1.12E+01	2.57E+00
CF4	Mean	8.42E+02	8.73E+02+	8.66E+02+	8.76E+02+	9.54E+02+	1.09E+03+	8.87E+02+	9.14E+02+	9.23E+02+	8.80E+02+	9.27E+02+	9.03E+02+
	Std	6.44E+00	1.81E+01	1.61E+01	1.77E+01	2.11E+01	2.36E+01	1.43E+01	2.66E+01	2.35E+01	2.23E+01	2.67E+01	3.45E+01
CF5	Mean	9.12E+02	1.89E+03+	1.78E+03+	1.85E+03+	3.26E+03+	9.79E+03+	2.28E+03+	3.68E+03+	2.80E+03+	2.07E+03+	3.55E+03+	2.73E+03+
	Std	4.97E+00	4.75E+02	9.71E+02	4.01E+02	8.00E+02	1.71E+03	3.79E+02	1.28E+03	5.83E+02	6.46E+02	1.04E+03	1.22E+03
CF6	Mean	1.96E+03	3.59E+03+	1.86E+06+	5.12E+03+	1.11E+09+	7.61E+09+	4.66E+03+	1.04E+07+	7.32E+05+	8.21E+03+	1.71E+06+	1.96E+07+
	Std	1.11E+02	1.99E+03	7.03E+06	5.09E+03	7.25E+08	2.47E+09	3.67E+03	3.03E+07	5.16E+05	6.41E+03	3.18E+06	1.11E+07
CF7	Mean	2.02E+03	2.07E+03+	2.16E+03+	2.10E+03+	2.23E+03+	2.45E+03+	2.15E+03+	2.18E+03+	2.12E+03+	2.12E+03+	2.19E+03+	2.09E+03+
	Std	4.32E+00	3.80E+01	7.21E+01	3.87E+01	7.90E+01	1.25E+02	6.95E+01	7.56E+01	2.35E+01	6.49E+01	6.39E+01	2.93E+01
CF8	Mean	2.22E+03	2.22E+03+	2.31E+03+	2.25E+03+	2.94E+03+	1.44E+04+	2.23E+03+	2.30E+03+	2.26E+03+	2.28E+03+	2.28E+03+	2.23E+03+
	Std	1.50E-01	4.97E+00	5.89E+01	4.35E+01	1.06E+03	1.91E+04	1.14E+01	7.72E+01	4.14E+01	6.33E+01	6.25E+01	5.43E+00
CF9	Mean	2.48E+03	2.49E+03+	2.50E+03+	2.48E+03-	3.01E+03+	3.92E+03+	2.48E+03-	2.56E+03+	2.54E+03+	2.54E+03+	2.57E+03+	2.49E+03+
	Std	9.77E-02	3.80E+00	3.81E+01	3.41E-02	1.77E+02	5.22E+02	5.53E-02	6.60E+01	4.14E+01	5.58E+01	5.48E+01	5.42E+00
CF10	Mean	2.50E+03	2.53E+03+	4.60E+03+	3.46E+03+	5.59E+03+	7.64E+03+	4.01E+03+	3.93E+03+	2.51E+03+	4.05E+03+	5.01E+03+	3.22E+03+
	Std	5.76E-02	6.70E+01	8.96E+02	1.16E+03	1.38E+03	1.05E+03	1.03E+03	8.34E+02	4.54E+01	1.31E+03	1.04E+03	7.34E+02
CF11	Mean	2.85E+03	2.93E+03+	2.99E+03+	2.90E+03≈	7.96E+03+	1.36E+04+	2.98E+03+	4.45E+03+	4.12E+03+	2.95E+03≈	3.67E+03+	3.46E+03+
	Std	1.14E+02	1.11E+02	3.75E+02	1.30E+02	9.07E+02	1.60E+03	1.10E+02	7.47E+02	3.44E+02	1.83E+02	1.10E+03	2.11E+02
CF12	Mean	2.94E+03	2.98E+03+	2.98E+03+	2.99E+03+	3.18E+03+	4.26E+03+	3.00E+03+	3.11E+03+	3.13E+03+	2.98E+03+	3.08E+03+	2.98E+03+
	Std	3.73E+00	1.62E+01	2.89E+01	4.94E+01	6.54E+01	3.42E+02	5.37E+01	7.92E+01	9.78E+01	2.24E+01	1.15E+02	3.36E+01
Chaos wins		+	12	11	9	12	12	11	12	12	11	12	12
Similar		≈	0	1	1	0	0	0	0	0	1	0	0
Competitor wins		-	0	0	2	0	0	1	0	0	0	0	0

Table 11. Statistical results of CEAHA compared with other optimization algorithms in CEC2022(20D).
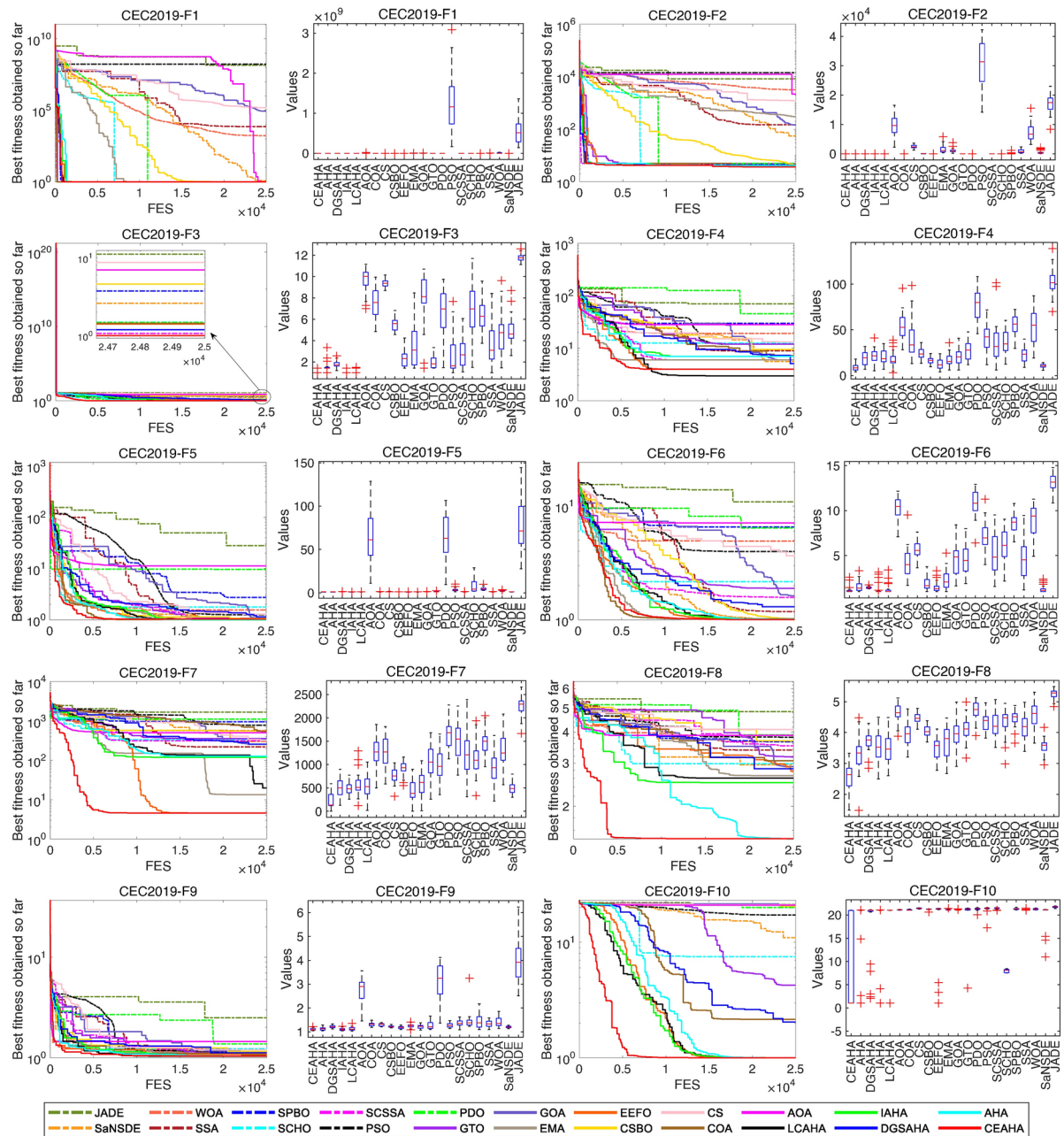
Figure 8. Fitness curves and box plots of CEAHA and other 21 algorithms used for comparative analysis on CEC2019.

achieved with other methods, this paper demonstrates the superiority of the proposed algorithm. In addressing these mechanical design issues, penalty functions are utilized to manage the various constraints, ensuring the generality and practicality of the algorithm. Specifically, suppose the optimization problem includes an objective function $f(X)$ and multiple constraints, including inequality constraints $g_i(X) \leq 0$ and equality constraints $h_i(X) = 0$, thereby allowing the construction of a new objective function $\Phi(X)$:

$$\Phi(X) = f(X) + \sum_{i=1}^{m} P_i \cdot \max(0, g_i(X)) + \sum_{j=1}^{n} Q_j \cdot |h_j(x)| \tag{21}$$

where, $f(X)$ represents the original objective function, $g_i(X)$ denotes the i-th inequality constraint, and $h_j(X)$ represents the j-th equality constraint. P_i and Q_i are the corresponding penalty coefficients, which reflect the severity of the penalty for violating each respective constraint. The detailed analyses of four constrained mechanical design problems are presented as follows.
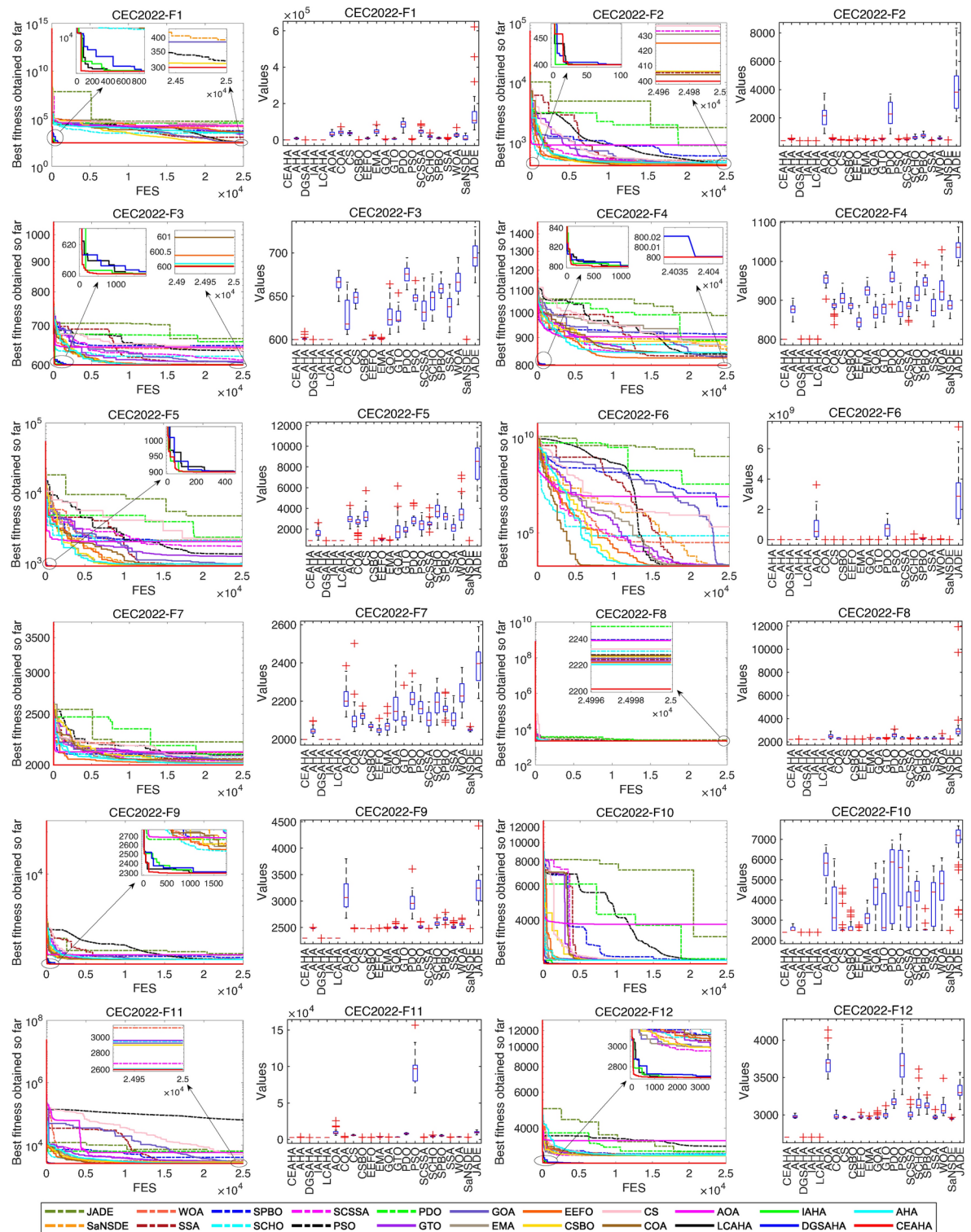
Figure 9. Fitness curves and box plots of CEAHA and other 21 algorithms used for comparative analysis on CEC2022 (20D).

Design of pressure vessel

The objective of this issue is to minimize the manufacturing cost of a pressure vessel, with its parameter structure illustrated in Fig. 12. The problem comprises 4 design variables (i.e., thickness of the shell (x_1), thickness of the head (x_2), inner radius (x_3), length of the cylindrical section of the vessel (x_4)). The penalty coefficient vector is denoted as $[P_1, P_2, P_3, P_4, Q] = [12{,}000, 8000, 1, 1, 1]$, with an additional constant constraint $h = 0$. The mathematical model of pressure vessel is as follows:
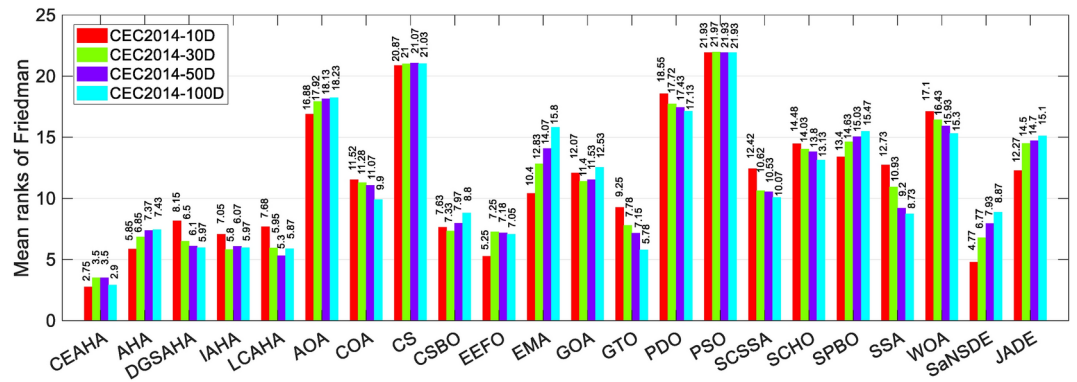
Figure 10. The column chart of Friedman's mean rank among CEAHA and other algorithms in CEC2014.
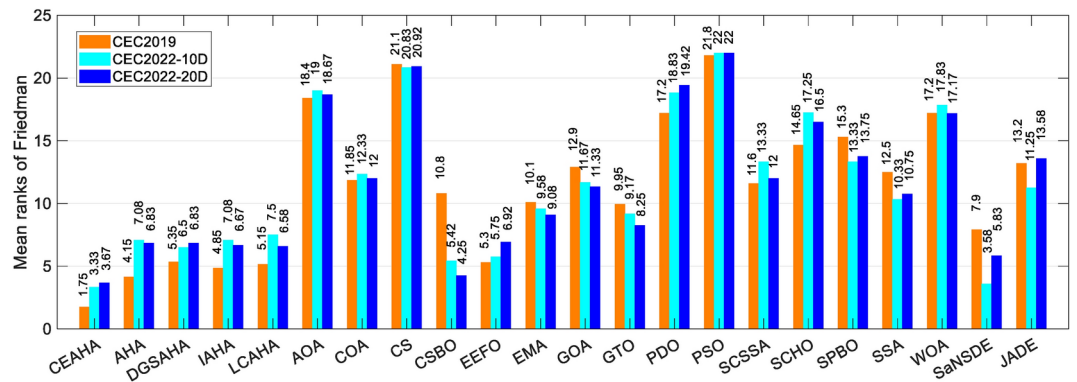
Figure 11. The column chart of Friedman's mean rank among CEAHA and other algorithms in CEC2019 and CEC2022.
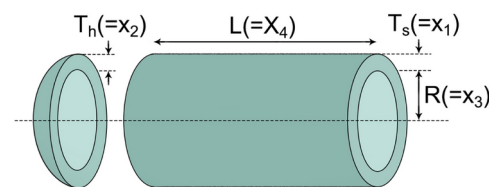
Figure 12. Structure of pressure vessel design problem.

Minimize:

$$f(X) = 0.6224x_1x_3x_4 + 1.7781x_2x_3^2 + 3.1661x_1^2x_4 + 19.84x_1^2x_3 \qquad (22)$$

Subject to:

$$\begin{cases} g_1(X) = -x_1 + 0.0193x_3 \leq 0 \\ g_2(X) = -x_2 + 0.00954x_4 \leq 0 \\ g_3(X) = -\pi x_3^2 x_4 - \frac{4}{3}\pi x_3^3 + 1{,}296{,}000 \leq 0 \\ g_4(X) = x_4 - 240 \leq 0 \end{cases} \qquad (23)$$

Among these variables, x_1 and x_2 are discrete, expressed as integer multiples of 0.0625. Conversely, x_3 and x_4 are continuous. Their respective lower and upper bounds specified below:

$$\begin{aligned} 1 \times 0.0625 \leq x_1, x_2 \leq 99 \times 0.0625, \\ 10 \leq x_3, x_4 \leq 200 \end{aligned} \qquad (24)$$

Algorithm	x_1	x_2	x_3	x_4	Best	Mean	Worst	Std
CEAHA (proposed)	0.8125	0.4375	42.09844560	176.63659584	**6059.714335**	6065.876708	6090.526201	12.5354
ISOS[6]	0.8125	0.4375	42.0984456	176.6365958	6059.714335	**6059.714335**	**6059.714335**	**0**
mSSA[7]	0.8125	0.4375	42.0984	176.6365	6059.714335	–	–	–
SNS[93]	0.8125	0.4375	42.09845	176.6366	6059.71434	6097.100294	6410.08689	92.8
AOA-NM[94]	0.8125	0.4375	42.09844	176.6365	6059.714335	6278.3193	6370.7797	258.368
GEA[95]	0.8125	0.4375	42.098445590	176.63659592	6059.714335	6084.727025	6371.338743	86.1
BBO[95]	0.8125	0.4375	42.09741762	176.65411485	6059.95129	6182.687452	6311.940267	147
RCGA[95]	0.8125	0.4375	42.09844559	176.63659592	6059.714335	6268.070258	6402.930865	217.6
CPSO[96]	0.8125	0.4375	42.0913	176.7465	6061.0777	6147.1332	6363.8041	86.5
MVO[97]	0.8125	0.4375	42.03149	177.4948	6068.5114	6465.6159	7335.9735	341.336
ASO[97]	0.8125	0.4375	41.89656	179.1544	6084.4534	6713.6637	7438.6515	320.651
EBO[97]	0.8125	0.4375	45.31918	140.4344	6092.5671	6501.0531	6830.7286	260.008
AOA[94]	0.8125	0.4375	45.33679	140.2538	6090.526	6583.0123	7274.452	424.753
AHA[43]	0.778171	0.384653	40.319674	199.999262	5885.35369	5885.53823	5885.8519	0.1378
LAA[98]	0.778195	0.385202	10.31993	200	5885.5773	–	–	–
mDE[99]	0.7791	0.3861	40.3682	199.3396	5886.661	5900.0005	6153.0972	0.010051
SCSO[100]	0.7798	0.9390	40.3864	199.2918	5917.46	–	–	–
WaOA[101]	0.778264	0.384775	40.32163	199.8713	5883.9604	–	–	–

Table 12. Statistical results of 30 independent runs of the pressure vessel design optimization problem. Significant values are given in bold.
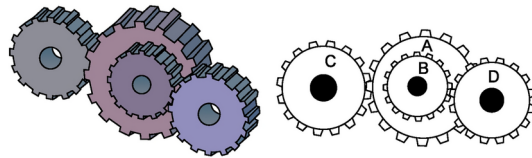
**Figure 13**. Structure of gear train design problem.

The solution results for this design challenge obtained by CEAHA and competing algorithms are displayed in Table 12. It can be observed that CEAHA, ISOS, mSSA, SNS, AOA-NM, GEA, and RCGA all have the potential to find the optimal solution; however, CEAHA achieves a lower mean solution value and a smaller standard deviation than SNS, AOA-NM, GEA, RCGA, and other competitors. It is worth noting that although the fitness function values obtained by AHA, LAA, mDE, SCSO, and WaOA are relatively small, these results are infeasible. The infeasibility arises because the design variables x_1 and x_2 they solved do not meet the discretization requirement of being integer multiples of 0.0625. Although CEAHA does not perform as well as ISOS in terms of mean and standard deviation when addressing the pressure vessel problem, it demonstrates a clear competitive advantage over other algorithms such as SNS, AOA-NM, GEA, BBO, RCGA, CPSO, MVO, ASO, EBO, and AOA, providing an effective new solution for solving the pressure vessel issue.

Design of gear train
The issue of gear train design (Fig. 13) represents an unconstrained discrete design problem within the field of mechanical engineering. The objective is to minimize the gear ratio, which is defined as the ratio of the angular velocity of the output shaft to that of the input shaft. Numbers of teeth on the gears, denoted as $n_A(= x_1)$, $n_B(= x_2)$, $n_C(= x_3)$ and $n_D(= x_4)$, are considered as design variables, with their mathematical model as follows:
Minimize:

$$f(X) = \left(\frac{1}{6.931} - \frac{x_3 x_2}{x_1 x_4} \right)^2 \tag{25}$$

Variable range:

$$x_i \in \{12, 13, 14, \dots, 60\}, i = 1, 2, 3, 4 \tag{26}$$

The penalty coefficient vector is denoted as $[P_1, P_2, P_3, Q] = [1, 1, 1, 1]$, with an additional constant constraint $h = 0$. Analysis of the data presented in Table 13 indicates that for the gear train design problem, CEAHA, SNS, GEA, ABC, and RCGA all have the potential to find the optimal solution across 30 independent runs.

Algorithms	n_A	n_B	n_C	n_D	Best	Mean	Worst	Std
CEAHA (proposed)	43	19	16	49	**2.700857E−12**	**9.49329054E−12**	**2.30781573E−11**	**9.77016762E−12**
SNS[93]	43	19	16	49	2.700857E−12	1.68012E−10	1.36165E−09	3.74894E−10
GEA[95]	43	16	19	49	2.700857E−12	3.392666E−10	9.92E−10	4.9E−10
ABC[95]	43	19	16	49	2.700857E−12	5.313982E−11	2.828166E−10	1.4E−9
RCGA[95]	43	19	16	49	2.700857E−12	1.2453314E−6	5.802142E−6	4.3E−6
BBO[95]	51	15	26	53	2.307816E−11	7.099246E−8	1.990372E−7	8.2E−7
GA[93]	49	19	16	43	2.7009E−12	1.6212E−09	1.5249E−08	3.2174E−09
PSO[93]	34	13	20	53	2.3078E−11	7.9383E−09	1.0222E−06	1.8147E−07
SSA[93]	–	–	–	–	2.7009E−12	1.9822E−09	2.7265E−08	4.5748E−09
WOA[93]	–	–	–	–	2.7009E−12	9.6633E−10	6.5123E−09	1.1296E−10
LAA[98]	39.4455	16.3337	12.002	34.4457	1.5049E−24	–	–	–

Table 13. Statistical results of 30 independent runs of the gear train design optimization problem. Significant values are given in bold.

Algorithms	b	m	Z	l_1	l_2	d_1	d_2	Best	Mean	Worst	Std
CEAHA (proposed)	3.5	0.7	17	7.3	7.71531991	3.35054095	5.28665446	**2994.42446576**	**2994.42446581**	**2994.42446591**	3.53188118E−08
mDE[99]	3.5	0.7	17	7.3	7.715319912	3.350540949	5.286654465	2994.424466	2994.424468	2994.424488	1.0011E−02
SNS[93]	3.5	0.7	17	7.3	7.71532	3.35021	5.28665	2994.4710696	2994.4710696	2994.4710992	7.00E−06
AHA[43]	–	–	–	–	–	–	–	2994.471158	2994.471652	2994.473229	4.2512E−4
LAA[98]	3.5002	0.7	17	7.3	7.7208	3.3516	5.28661	2994.662	–	–	–
EABOA[102]	3.5	0.7	17	7.3	7.715	3.351	5.287	2994.5422	2994.55422	–	**9.15E-13**
AOA[98]	3.5611	0.7	17	7.3	7.8131	3.4165	5.28828	3004.65	–	–	–
WaOA[101]	3.5	0.700007	17	7.3	7.8	3.350209	5.286683	2996.3482	–	–	–
CS[93]	3.5	0.7	17	7.605	7.8181	3.352	5.2875	3000.981	3007.1997	3009	4.96E+00
ABC[93]	3.5	0.7	17	7.3	7.8	3.35022	5.28668	2997.058412	2997.058412	–	0.00E+00
APSO[93]	3.50159	0.7	17	7.3	7.8	3.35127	5.28874	3187.630486	3822.640624	4443.017639	3.66E+02
WOA[93]	–	–	–	–	–	–	–	2996.60434	3042.915023	3233.598124	4.08E+01
SSA[93]	–	–	–	–	–	–	–	2996.02172	3005.574377	3015.662612	4.63E+00
PSO[99]	3.5015	0.7	17	7.605	7.8181	3.352	5.2875	3000.981	3005.254	3007.019	4.2511E+00
DE[93]	3.5	0.7	17	7.3	7.8	3.3502	5.2867	2996.349	2998.217	2999.24	2.0147E−01

Table 14. Statistical results of 30 independent runs of the speed reducer design optimization problem. Significant values are given in bold.
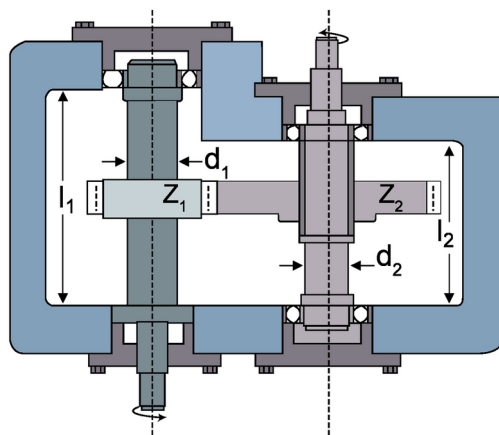
Figure 14. Structure of speed reducer problem.
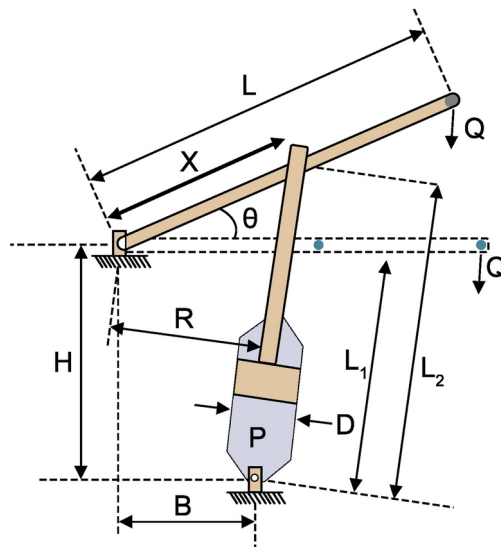
Figure 15. Structure of piston lever problem.

However, CEAHA exhibited the best average performance among all the algorithms and the least standard deviation, demonstrating higher efficiency and stability in solving this design challenge. It is worth noting that although LAA achieves relatively low fitness function values, these results are infeasible. The reason is that the design variables n_A, n_B, n_C, and n_D solved by LAA do not meet the requirements for discretization into positive integers.

Design of speed reducer

The speed reducer (Fig. 14) is a crucial component of the gearbox, applicable to a variety of uses. The weight of the reducer will be minimized under 11 constraint conditions. The problem involves seven variables: the width of the tooth surface $b(= x_1)$, the module of the tooth surface $m(= x_2)$, the number of teeth in the small gear $z(= x_3)$, the length of the first shaft between bearings $l_1(= x_4)$, the length of the second shaft between bearings $l_2(= x_5)$, the diameter of the first shaft $d_1(= x_6)$ and the diameter of the second shaft $d_2(= x_7)$. The penalty coefficient vector is denoted as $[P_1, P_2, \ldots, P_{11}, Q] = [50, 10, 1, 1, 1, 20, 1, 300, 1, 1, 50, 1]$, with an additional constant constraint $h = 0$. The mathematical formulas for this problem are as follows:

Minimize:

$$f(X) = 0.7845x_1x_2^2(3.3333x_3^2 + 14.9334x_3 - 43.0934) - 1.508x_1(x_6^2 + x_7^2) + 7.4777(x_6^3 + x_7^3) + 0.7854(x_4x_6^2 + x_5x_7^2) \quad (27)$$

Subject to:

$$g_1(X) = \frac{27}{x_1x_2^2x_3} - 1 \le 0 \quad (28)$$

$$g_2(X) = \frac{397.5}{x_1x_2^2x_3^2} - 1 \le 0 \quad (29)$$

$$g_3(X) = \frac{1.93x_4^3}{x_2x_6^4x_3} - 1 \le 0 \quad (30)$$

$$g_4(X) = \frac{1.93x_5^3}{x_2x_7^4x_3} - 1 \le 0 \quad (31)$$

$$g_5(X) = \frac{\sqrt{(745x_4/(x_2x_3))^2 + 16.9 \times 10^6}}{110x_6^3} - 1 \le 0 \quad (32)$$

$$g_6(X) = \frac{\sqrt{(745x_5/(x_2x_3))^2 + 157.5 \times 10^6}}{85x_7^3} - 1 \le 0 \quad (33)$$

$$g_7(X) = \frac{x_2x_3}{40} - 1 \le 0 \quad (34)$$

$$g_8(X) = \frac{5x_2}{x_1} - 1 \le 0 \tag{35}$$

$$x_9(X) = \frac{x_1}{12x_2} - 1 \le 0 \tag{36}$$

$$g_{10}(X) = \frac{1.5x_6 + 1.9}{x_4} - 1 \le 0 \tag{37}$$

$$g_{11}(X) = \frac{1.1x_7 + 1.9}{x_5} - 1 \le 0 \tag{38}$$

Variable range:

$$
\begin{aligned}
2.6 &\le x_1 \le 3.6 \\
0.7 &\le x_2 \le 0.8 \\
x_3 &\in \{17.18.19, \ldots, 28\} \\
7.3 &\le x_4, x_5 \le 8.3 \\
2.9 &\le x_6 \le 3.9 \\
5.0 &\le x_7 \le 5.5
\end{aligned}
\tag{39}
$$

Analysis of the data from Table 14 reveals that in addressing the gear train design problem, CEAHA, mDE, SNS, AHA, and EABOA all have the potential to find the optimal solution in 30 independent runs. However, CEAHA demonstrates the best average performance among all the algorithms. Although EABOA exhibits the smallest variance in the context of gearbox design optimization, its ability to find the optimal solution is inferior to that of CEAHA.

Design of piston lever
The primary objective of this problem is to minimize the itinerary when raising the piston lever from $0°$ to $45°$, by positioning components $H(= x_1)$, $B(= x_2)$, $D(= x_3)$ and $X(= x_4)$ of the piston lever (Fig. 15). The penalty coefficient vector is denoted as $[P_1, P_2, P_3, P_4, Q] = [1, 1, 1, 100, 1]$, with an additional constant constraint $h = 0$. The mathematical formulas for the problem are as follows:
  Minimize:

$$f(X) = \tfrac{1}{4}\pi x_3^2 (L_2 - L_1) \tag{40}$$

Subject to:

$$g_1(X) = QL\cos\theta - R \times F \le 0 \tag{41}$$

$$g_2(X) = Q(L - x_4) - M_{\max} \le 0 \tag{42}$$

$$g_3(X) = 1.2(L_2 - L_1) - L_1 \le 0 \tag{43}$$

$$g_4(X) = \frac{x_3}{2} - x_2 \le 0 \tag{44}$$

where,

$$
\begin{aligned}
R &= \frac{|-x_4(x_4\sin\theta + x_1) + x_1(x_2 - x_4\cos\theta)|}{\sqrt{(x_4 - x_2)^2 + x_1^2}} \\
F &= \frac{\pi P x_3^2}{4} \\
L_1 &= \sqrt{(x_4 - x_2)^2 + x_1^2} \\
L_2 &= \sqrt{(x_4\sin\theta + x_1)^2 + (x_2 - x_4\cos\theta)^2} \\
\theta &= 45° \\
Q &= 10,000\,lbs \\
L &= 240\,in \\
M_{\max} &= 1.8 \times 10^6\,lbsin \\
P &= 1500\,psi
\end{aligned}
\tag{45}
$$

Variable range:

Algorithms	H	B	D	X	Best	Mean	Worst	Std
CEAHA (proposed)	0.05	2.04151363	4.08302719	120	8.41269854	**8.41270031**	**8.41270579**	**2.07382E−06**
SNS[93]	0.05	2.042	120	4.083	**8.412698349**	24.3189743	167.4727747	47.71792646
AOA-NM[94]	0.05	2.04151359	120	4.08302718	8.41269883	76.5369	158.6359	36.5321
EBO[97]	0.05	2.0415137	120	4.0830272	8.4126988	110.9658	181.5427	75.0184
MGA[93]	–	–	–	–	8.413406652	32.4688925	167.4732134	29.96370439
MVO[97]	0.05	2.045092671	120	4.083549433	8.428996054	138.4470	356.2368	138.5046
SSA[94]	0.05	2.042281006	119.9111921	4.084534997	8.422037847	276.9405	653.4973	121.4145
CS[93]	0.05	2.043	120	4.085	8.4271	40.2319	168.592	59.0552
ASO[97]	415.704449	443.265522	63.3444604	2.43805252	213.834591	346.0264	778.6031	115.1357
AOA[94]	0.05	2.14889	110.644	4.24721	9.57467	180.0112	428.547	118.023
PSO[93]	133.3	2.44	117.14	4.75	122	166	294	51.7
DE[93]	129.4	2.43	119.8	4.75	159	187	199	14.2

Table 15. Statistical results of 30 independent runs of the piston lever design optimization problem. Significant values are given in bold.

$$0.05 \leq x_1, x_2, x_4 \leq 500$$
$$0.05 \leq x_3 \leq 200$$

(46)

An analysis of the data in Table 15 indicates that, when addressing the piston lever design problem, the algorithms CEAHA, SNS, AOA-NM, EBO, and MVO all exhibit the potential to find the optimal solution across 30 independent runs. However, CEAHA has demonstrated exceptional average optimization performance and lower standard deviations. Although the best fitness value of SNS is slightly lower than that of CEAHA, CEAHA outperforms SNS in terms of mean, worst-case performance, and standard deviation. This suggests that CEAHA exhibits greater robustness in the context of piston lever design optimization.

It can be observed from these four mechanical design problems, characterized by composite constraints, that CEAHA not only possesses commendable average performance but also exhibits excellent robustness, capable of achieving cost-minimized solutions with limited computational resources.

Conclusions

In this study, the ergodic chaotic motion mechanism is applied within the artificial hummingbird algorithm (AHA) framework to develop an enhanced version, termed CEAHA, which incorporates chaotic traversal flight. This study introduces the concept of traversal efficiency by chaotic intelligent entities within the solution space for the first time, and examines the impact of eight chaotic maps capable of generating centrally symmetric distributions on the convergence speed and population diversity of optimization algorithms. It is shown that the Cubic mapping significantly aids algorithmic agents in escaping local optima. This paper provides an in-depth analysis of the global search role of the Tent mapping with an invariant probability measure of 1 and the benefits of the U-shaped Cubic mapping in escaping local optima, enhancing population diversity, and comprehensively exploiting the solution space. By integrating chaotic dynamics, CEAHA effectively synergizes exploration and exploitation in optimization processes. Performance evaluations on 23 standard test functions, the CEC2014 and CEC2019 test suites, the latest single-objective test suite CEC2022, and four mechanical design cases (including pressure vessel, gear train, speed reducer, and piston lever designs) demonstrate CEAHA's exceptional convergence capabilities and robustness. These findings underscore the substantial potential for including chaotic mappings in meta-heuristic optimization algorithm design. Additionally, the deterministic nature of chaos, with its inherent randomness, is well-suited to population movement patterns and is expected to significantly improve metaheuristic algorithms' performance in solving complex optimization problems through accelerated convergence, enhanced solution quality, and reduced resource consumption. However, for specific scenarios, how to combine different chaotic motion laws to design diverse chaotic optimization strategies to adapt to various optimization tasks remains an urgent topic for exploration.

Data availability

All data generated or analyzed during this study are included directly in the text of this submitted manuscript. There are no additional external files with datasets.

References

1. Niu, Y., Yan, X., Wang, Y. & Niu, Y. 3d real-time dynamic path planning for uav based on improved interfered fluid dynamical system and artificial neural network. *Adv. Eng. Inform.* **59**, 102306 (2024).
2. Jin, W. et al. Enhanced uav pursuit-evasion using boids modelling: A synergistic integration of bird swarm intelligence and drl. *Comput. Mater. Contin.* **80** (2024).

3. Xu, X., Lin, Z., Li, X., Shang, C. & Shen, Q. Multi-objective robust optimisation model for mdvrpls in refined oil distribution. *Int. J. Prod. Res.* **60**, 6772–6792 (2022).
4. Çelik, E. Iegqo-aoa: information-exchanged gaussian arithmetic optimization algorithm with quasi-opposition learning. *Knowl.-Based Syst.* **260**, 110169 (2023).
5. Çelik, E. Improved stochastic fractal search algorithm and modified cost function for automatic generation control of interconnected electric power systems. *Eng. Appl. Artif. Intell.* **88**, 103407 (2020).
6. Çelik, E. A powerful variant of symbiotic organisms search algorithm for global optimization. *Eng. Appl. Artif. Intell.* **87**, 103294 (2020).
7. Çelik, E., Öztürk, N. & Arya, Y. Advancement of the search process of salp swarm algorithm for global optimization problems. *Expert Syst. Appl.* **182**, 115292 (2021).
8. Abualigah, L. et al. Meta-heuristic optimization algorithms for solving real-world mechanical engineering design problems: a comprehensive survey, applications, comparative analysis, and results. *Neural Comput. Appl.* 1–30 (2022).
9. Rajwar, K., Deep, K. & Das, S. An exhaustive review of the metaheuristic algorithms for search and optimization: taxonomy, applications, and open challenges. *Artif. Intell. Rev.* **56**, 13187–13257 (2023).
10. Alhijawi, B. & Awajan, A. Genetic algorithms: Theory, genetic operators, solutions, and applications. *Evol. Intel.* **17**, 1245–1256 (2024).
11. Ahmad, M. F., Isa, N. A. M., Lim, W. H. & Ang, K. M. Differential evolution: A recent review based on state-of-the-art works. *Alex. Eng. J.* **61**, 3831–3872 (2022).
12. Im, J., Rizzo, C. B., de Barros, F. P. & Masri, S. F. Application of genetic programming for model-free identification of nonlinear multi-physics systems. *Nonlinear Dyn.* **104**, 1781–1800 (2021).
13. Sulaiman, M. H., Mustaffa, Z., Saari, M. M., Daniyal, H. & Mirjalili, S. Evolutionary mating algorithm. *Neural Comput. Appl.* **35**, 487–516 (2023).
14. Zhong, J., Feng, L. & Ong, Y.-S. Gene expression programming: A survey. *IEEE Comput. Intell. Mag.* **12**, 54–72 (2017).
15. Yang, Z., Tang, K. & Yao, X. Self-adaptive differential evolution with neighborhood search. In *2008 IEEE congress on evolutionary computation (IEEE World Congress on Computational Intelligence)*, 1110–1116 (IEEE, 2008).
16. Zhang, J. & Sanderson, A. C. Jade: adaptive differential evolution with optional external archive. *IEEE Trans. Evol. Comput.* **13**, 945–958 (2009).
17. Hashemi, A., Dowlatshahi, M. B. & Nezamabadi-Pour, H. Gravitational search algorithm: Theory, literature review, and applications. *Handb. AI-Based Metaheuristics* 119–150 (2021).
18. Mirjalili, S., Mirjalili, S. M. & Hatamlou, A. Multi-verse optimizer: a nature-inspired algorithm for global optimization. *Neural Comput. Appl.* **27**, 495–513 (2016).
19. Karami, H., Anaraki, M. V., Farzin, S. & Mirjalili, S. Flow direction algorithm (fda): a novel optimization approach for solving optimization problems. *Comput. Ind. Eng.* **156**, 107224 (2021).
20. Kaveh, A. & Khayatazad, M. A new meta-heuristic method: ray optimization. *Comput. Struct.* **112**, 283–294 (2012).
21. Fallah, A. M. et al. Novel neural network optimized by electrostatic discharge algorithm for modification of buildings energy performance. *Sustainability* **15**, 2884 (2023).
22. Hashim, F. A., Houssein, E. H., Mabrouk, M. S., Al-Atabany, W. & Mirjalili, S. Henry gas solubility optimization: A novel physics-based algorithm. *Futur. Gener. Comput. Syst.* **101**, 646–667 (2019).
23. Wei, Z., Huang, C., Wang, X., Han, T. & Li, Y. Nuclear reaction optimization: A novel and powerful physics-based algorithm for global optimization. *IEEE Access* **7**, 66084–66109 (2019).
24. Erol, O. K. & Eksin, I. A new optimization method: big bang-big crunch. *Adv. Eng. Softw.* **37**, 106–111 (2006).
25. Bai, J. et al. A sinh cosh optimizer. *Knowl.-Based Syst.* **282**, 111081 (2023).
26. Izci, D. et al. Refined sinh cosh optimizer tuned controller design for enhanced stability of automatic voltage regulation. *Electr. Eng.* 1–14 (2024).
27. Yadav, R. & Kaur, M. Teaching learning based optimization-a review on background and development. In *AIP Conference Proceedings*, vol. 2986 (AIP Publishing, 2024).
28. Mousavirad, S. J. & Ebrahimpour-Komleh, H. Human mental search: a new population-based metaheuristic optimization algorithm. *Appl. Intell.* **47**, 850–887 (2017).
29. Kashan, A. H. League championship algorithm (lca): An algorithm for global optimization inspired by sport championships. *Appl. Soft Comput.* **16**, 171–200 (2014).
30. Elyasi, M., Selcuk, Y. S., Özener, O. Ö. & Coban, E. Imperialist competitive algorithm for unrelated parallel machine scheduling with sequence-and-machine-dependent setups and compatibility and workload constraints. *Comput. Ind. Eng.* **190**, 110086 (2024).
31. Lian, J. & Hui, G. Human evolutionary optimization algorithm. *Expert Syst. Appl.* **241**, 122638 (2024).
32. Das, B., Mukherjee, V. & Das, D. Student psychology based optimization algorithm: A new population based optimization algorithm for solving optimization problems. *Adv. Eng. Softw.* **146**, 102804 (2020).
33. Zhu, B. et al. A critical scenario search method for intelligent vehicle testing based on the social cognitive optimization algorithm. *IEEE Trans. Intell. Transp. Syst.* **24**, 7974–7986 (2023).
34. Ghasemi, M. et al. Circulatory system based optimization (csbo): an expert multilevel biologically inspired meta-heuristic algorithm. *Eng. Appl. Comput. Fluid Mech.* **16**, 1483–1525 (2022).
35. Nayak, J., Swapnarekha, H., Naik, B., Dhiman, G. & Vimal, S. 25 years of particle swarm optimization: Flourishing voyage of two decades. *Arch. Comput. Methods Eng.* **30**, 1663–1725 (2023).
36. Rana, N., Latiff, M. S. A., Abdulhamid, S. M. & Chiroma, H. Whale optimization algorithm: a systematic review of contemporary applications, modifications and developments. *Neural Comput. Appl.* **32**, 16245–16277 (2020).
37. Zhao, W. et al. Electric eel foraging optimization: A new bio-inspired optimizer for engineering applications. *Expert Syst. Appl.* **238**, 122200 (2024).
38. Demir, A. et al. Solving optimization problems via vortex optimization algorithm and cognitive development optimization algorithm. In *BRAIN. Broad Research in Artificial Intelligence and Neuroscience* 7, 23–42 (2017).
39. Meraihi, Y., Gabis, A. B., Mirjalili, S. & Ramdane-Cherif, A. Grasshopper optimization algorithm: theory, variants, and applications. *Ieee Access* **9**, 50001–50024 (2021).
40. Abualigah, L., Shehab, M., Alshinwan, M. & Alabool, H. Salp swarm algorithm: a comprehensive survey. *Neural Comput. Appl.* **32**, 11195–11215 (2020).
41. Abdollahzadeh, B., Soleimanian Gharehchopogh, F. & Mirjalili, S. Artificial gorilla troops optimizer: a new nature-inspired metaheuristic algorithm for global optimization problems. *Int. J. Intell. Syst.* **36**, 5887–5958 (2021).
42. Jia, H., Rao, H., Wen, C. & Mirjalili, S. Crayfish optimization algorithm. *Artif. Intell. Rev.* **56**, 1919–1979 (2023).
43. Zhao, W., Wang, L. & Mirjalili, S. Artificial hummingbird algorithm: A new bio-inspired optimizer with its engineering applications. *Comput. Methods Appl. Mech. Eng.* **388**, 114194 (2022).
44. Abd El-Sattar, H., Kamel, S., Hassan, M. H. & Jurado, F. An effective optimization strategy for design of standalone hybrid renewable energy systems. *Energy* **260**, 124901 (2022).
45. Kansal, V. & Dhillon, J. Ameliorated artificial hummingbird algorithm for coordinated wind-solar-thermal generation scheduling problem in multiobjective framework. *Appl. Energy* **326**, 120031 (2022).

46. Essa, F. A., Abd Elaziz, M., Al-Betar, M. A. & Elsheikh, A. H. Performance prediction of a reverse osmosis unit using an optimized long short-term memory model by hummingbird optimizer. *Process Saf. Environ. Protect.* **169**, 93–106 (2023).

47. Hu, G., Zhong, J., Zhao, C., Wei, G. & Chang, C.-T. Lcaha: A hybrid artificial hummingbird algorithm with multi-strategy for engineering applications. *Comput. Methods Appl. Mech. Eng.* **415**, 116238 (2023).

48. Zelinka, I. & Richter, H. *Evolutionary Algorithms for Chaos Researchers, 37–88* (Springer, Berlin Heidelberg, Berlin, Heidelberg, 2010).

49. Aditya, N. & Mahapatra, S. S. Switching from exploration to exploitation in gravitational search algorithm based on diversity with chaos. *Inf. Sci.* **635**, 298–327 (2023).

50. Zhao, Y., Dong, J., Li, X., Chen, H. & Li, S. A binary dandelion algorithm using seeding and chaos population strategies for feature selection. *Appl. Soft Comput.* **125**, 109166 (2022).

51. Oueslati, R., Manita, G., Chhabra, A. & Korbaa, O. Chaos game optimization: A comprehensive study of its variants, applications, and future directions. *Comput. Sci. Rev.* **53**, 100647 (2024).

52. Strogatz, S. H. *Nonlinear dynamics and chaos: with applications to physics, biology, chemistry, and engineering* (CRC press, 2018).

53. Tian, H. et al. Dynamic analysis and sliding mode synchronization control of chaotic systems with conditional symmetric fractional-order memristors. *Fractal and Fract.* **8**, 307 (2024).

54. Caponetto, R., Fortuna, L., Fazzino, S. & Xibilia, M. G. Chaotic sequences to improve the performance of evolutionary algorithms. *IEEE Trans. Evol. Comput.* **7**, 289–304 (2003).

55. Li, M., Kang, H. & Zhou, P. Hybrid optimization algorithm based on chaos, cloud and particle swarm optimization algorithm. *J. Syst. Eng. Electron.* **24**, 324–334 (2013).

56. Rosić, M., Sedak, M., Simić, M. & Pejović, P. Chaos-enhanced adaptive hybrid butterfly particle swarm optimization algorithm for passive target localization. *Sensors* **22**, 5739 (2022).

57. Chu, H., Yi, J. & Yang, F. Chaos particle swarm optimization enhancement algorithm for uav safe path planning. *Appl. Sci.* **12**, 8977 (2022).

58. Jiang, B. L. W. Optimizing complex functions by chaos search. *Cybern. Syst.* **29**, 409–419 (1998).

59. Rim, C., Piao, S., Li, G. & Pak, U. A niching chaos optimization algorithm for multimodal optimization. *Soft. Comput.* **22**, 621–633 (2018).

60. Yang, D., Liu, Z. & Yi, P. Computational efficiency of accelerated particle swarm optimization combined with different chaotic maps for global optimization. *Neural Comput. Appl.* **28**, 1245–1264 (2017).

61. Thoa, T. T. & Pei, Y. An analysis of optimization performance on chaotic evolution algorithm using multiple chaotic systems with elite strategy. In *2021 IEEE International Conference on Systems, Man, and Cybernetics (SMC)*, 649–654 (IEEE, 2021).

62. Rauf, H. T. et al. Multi population-based chaotic differential evolution for multi-modal and multi-objective optimization problems. *Appl. Soft Comput.* **132**, 109909 (2023).

63. Abdelrazek, M., Abd Elaziz, M. & El-Baz, A. Cdmo: Chaotic dwarf mongoose optimization algorithm for feature selection. *Sci. Rep.* **14**, 701 (2024).

64. Mohamed, A. A., Kamel, S., Hassan, M. H. & Zeinoddini-Meymand, H. Cavoa: A chaotic optimization algorithm for optimal power flow with facts devices and stochastic wind power generation. *IET Gen. Transm. Distrib.* **18**, 121–144 (2024).

65. Yıldız, B. S., Mehta, P., Panagant, N., Mirjalili, S. & Yildiz, A. R. A novel chaotic Runge Kutta optimization algorithm for solving constrained engineering problems. *J. Comput. Des. Eng.* **9**, 2452–2465 (2022).

66. Wolpert, D. H. & Macready, W. G. No free lunch theorems for optimization. *IEEE Trans. Evol. Comput.* **1**, 67–82 (1997).

67. Wang, J., Li, Y., Hu, G. & Yang, M. An enhanced artificial hummingbird algorithm and its application in truss topology engineering optimization. *Adv. Eng. Inform.* **54**, 101761 (2022).

68. Wang, L., Zhang, L., Zhao, W. & Liu, X. Parameter identification of a governing system in a pumped storage unit based on an improved artificial hummingbird algorithm. *Energies* **15**, 6966 (2022).

69. Kaur, G. & Arora, S. Chaotic whale optimization algorithm. *J. Comput. Des. Eng.* **5**, 275–284 (2018).

70. Yang, W. et al. Pm 2.5 concentration prediction in lanzhou, china, using hyperchaotic cuckoo search-extreme learning machine. *Stoch. Environ. Res. Risk Assessment* **37**, 261–273 (2023).

71. Naanaa, A. Fast chaotic optimization algorithm based on spatiotemporal maps for global optimization. *Appl. Math. Comput.* **269**, 402–411 (2015).

72. Fu, Y., Liu, D., Fu, S., Chen, J. & He, L. Enhanced aquila optimizer based on tent chaotic mapping and new rules. *Sci. Rep.* **14**, 3013 (2024).

73. Huang, H., Yao, Z., Wei, X. & Zhou, Y. Twin support vector machines based on chaotic mapping dung beetle optimization algorithm. *J. Comput. Des. Eng.* **11**, 101–110 (2024).

74. Yang, D., Li, G. & Cheng, G. On the efficiency of chaos optimization algorithms for global optimization. *Chaos Solitons Fract.* **34**, 1366–1375 (2007).

75. Yang, D., Liu, Z. & Zhou, J. Chaos optimization algorithms based on chaotic maps with different probability distribution and search speed for global optimization. *Commun. Nonlinear Sci. Numer. Simul.* **19**, 1229–1246 (2014).

76. Aydemir, S. B. A novel arithmetic optimization algorithm based on chaotic maps for global optimization. *Evol. Intel.* **16**, 981–996 (2023).

77. Zheng, S., Zou, F. & Chen, D. Sparrow search algorithm based on cubic mapping and its application. In *International Conference on Intelligent Computing*, 376–385 (Springer, 2023).

78. Wu, D., Zhang, X., Wang, J., Li, L. & Feng, G. Novel robust video watermarking scheme based on concentric ring subband and visual cryptography with piecewise linear chaotic mapping. *IEEE Trans. Circ. Syst. Video Technol.* (2024).

79. Natiq, H., Banerjee, S., He, S., Said, M. & Kilicman, A. Designing an m-dimensional nonlinear model for producing hyperchaos. *Chaos Solitons Fract.* **114**, 506–515 (2018).

80. Wang, Y., Wang, T., Dong, S. & Yao, C. An improved grey-wolf optimization algorithm based on circle map. In *Journal of Physics: Conference Series*, vol. 1682, 012020 (IOP Publishing, 2020).

81. Zhang, M., Wang, D. & Yang, J. Hybrid-flash butterfly optimization algorithm with logistic mapping for solving the engineering constrained optimization problems. *Entropy* **24**, 525 (2022).

82. Rudnicki, R. An ergodic theory approach to chaos. *Discrete Contin. Dynam. Systems* **35**, 2015 (2015).

83. Mitkowski, P. J. *Chaos and Ergodic Theory, 19–40* (Springer International Publishing, Cham, 2021).

84. Civicioglu, P. & Besdok, E. Colony-based search algorithm for numerical optimization. *Appl. Soft Comput.* **151**, 111162 (2024).

85. Deng, X., He, D. & Qu, L. A multi-strategy enhanced arithmetic optimization algorithm and its application in path planning of mobile robots. *Neural Process. Lett.* **56**, 18 (2024).

86. Aditya, N. & Mahapatra, S. S. Switching from exploration to exploitation in gravitational search algorithm based on diversity with chaos. *Inf. Sci.* **635**, 298–327 (2023).

87. Mariprasath, T., Basha, C. H., Khan, B. & Ali, A. A novel on high voltage gain boost converter with cuckoo search optimization based mpptcontroller for solar pv system. *Sci. Rep.* **14**, 8545 (2024).

88. Abualigah, L., Diabat, A., Mirjalili, S., Abd Elaziz, M. & Gandomi, A. H. The arithmetic optimization algorithm. *Comput. Methods Appl. Mech. Eng.* **376**, 113609 (2021).

89. Ezugwu, A. E., Agushaka, J. O., Abualigah, L., Mirjalili, S. & Gandomi, A. H. Prairie dog optimization algorithm. *Neural Comput. Appl.* **34**, 20017–20065 (2022).

90. Li, A., Quan, L., Cui, G. & Xie, S. Sparrow search algorithm combining sine-cosine and cauchy mutation. *Comput. Eng. Appl.* **58**, 91–99 (2022).
91. Derrac, J., García, S., Molina, D. & Herrera, F. A practical tutorial on the use of nonparametric statistical tests as a methodology for comparing evolutionary and swarm intelligence algorithms. *Swarm Evol. Comput.* **1**, 3–18 (2011).
92. Raj, S. et al. A novel chaotic chimp sine cosine algorithm part-i: For solving optimization problem. *Chaos Solitons Fract.* **173**, 113672 (2023).
93. Bayzidi, H., Talatahari, S., Saraee, M. & Lamarche, C.-P. Social network search for solving engineering optimization problems. *Comput. Intell. Neurosci.* **2021**, 8548639 (2021).
94. Yıldız, B. S. et al. A novel hybrid arithmetic optimization algorithm for solving constrained optimization problems. *Knowl.-Based Syst.* **271**, 110554 (2023).
95. Ghasemi, M. et al. Geyser inspired algorithm: a new geological-inspired meta-heuristic for real-parameter and constrained engineering optimization. *J. Bionic Eng.* **21**, 374–408 (2024).
96. He, Q. & Wang, L. An effective co-evolutionary particle swarm optimization for constrained engineering design problems. *Eng. Appl. Artif. Intell.* **20**, 89–99 (2007).
97. Dhal, K. G., Sasmal, B., Das, A., Ray, S. & Rai, R. A comprehensive survey on arithmetic optimization algorithm. *Arch. Comput. Methods Eng.* **30**, 3379–3404 (2023).
98. Barua, S. & Merabet, A. Lévy arithmetic algorithm: An enhanced metaheuristic algorithm and its application to engineering optimization. *Expert Syst. Appl.* **241**, 122335 (2024).
99. Tiwari, P., Mishra, V. N. & Parouha, R. P. Developments and design of differential evolution algorithm for non-linear/non-convex engineering optimization. *Arch. Comput. Methods Eng.* **31**, 2227–2263 (2024).
100. Seyyedabbasi, A. & Kiani, F. Sand cat swarm optimization: A nature-inspired algorithm to solve global optimization problems. *Eng. Comput.* **39**, 2627–2651 (2023).
101. Trojovský, P. & Dehghani, M. A new bio-inspired metaheuristic algorithm for solving optimization problems based on walruses behavior. *Sci. Rep.* **13**, 8775 (2023).
102. He, K., Zhang, Y., Wang, Y.-K., Zhou, R.-H. & Zhang, H.-Z. Eaboa: Enhanced adaptive butterfly optimization algorithm for numerical optimization and engineering design problems. *Alex. Eng. J.* **87**, 543–573 (2024).

Acknowledgements

Author contributions

Conceptualization, J.D. and J.Z.; methodology, J.D., J.Z. and S.L.; software, J.D.; validation, J.Z., S.L. and Z.Y.; formal analysis, S.L.; investigation, J.Z., S.L. and Z.Y.; resources, J.D.; data curation, J.Z.; writing—original draft preparation, J.D. and J.Z; writing—review and editing, J.Z., S.L. and Z.Y.; visualization, J.Z.; supervision, J.D. and S.L.; project administration, J.D. and S.L.; funding acquisition, J.D. and S.L. All authors have read and agreed to the published version of the manuscript.

Declarations

Competing interests

The authors declare that they have no known competing financial interests or personal relationships that could have appeared to influence the work reported in this paper.

Additional information

Correspondence and requests for materials should be addressed to J.Z.

Reprints and permissions information is available at www.nature.com/reprints.

Publisher's note Springer Nature remains neutral with regard to jurisdictional claims in published maps and institutional affiliations.